(12) INTERNATIONAL APPLICATION PUBLISHED UNDER THE PATENT COOPERATION TREATY (PCT)

(19) World Intellectual Property Organization
International Bureau

(43) International Publication Date
27 May 2004 (27.05.2004)

PCT

(10) International Publication Number
WO 2004/044249 A2

(51) International Patent Classification[7]: C21D

(21) International Application Number:
PCT/US2003/035575

(22) International Filing Date:
10 November 2003 (10.11.2003)

(25) Filing Language: English

(26) Publication Language: English

(30) Priority Data:
60/425,964 13 November 2002 (13.11.2002) US

(71) Applicant *(for all designated States except US)*: **IOWA STATE UNIVERSITY RESEARCH FOUNDATION, INC.** [US/US]; 310 Lab of Mechanics, Ames, IO 50011-2131 (US).

(72) Inventors; and

(75) Inventors/Applicants *(for US only)*: **GSCHNEIDNER, Karl, A., Jr.** [US/US]; 2215 Duff, Ames, IA 50010 (US). **PECHARSKY, Alexandra, O.** [US/US]; 2621 Green Hills Drive, Ames, IA 50014 (US). **PECHARSKY, Vitalij, K.** [US/US]; 2621 Green Hills Drive, Ames, IA 50014 (US). **RUSSELL, Alan, M.** [US/US]; 1713 Amherst Drive, Ames IA 50014 (US).

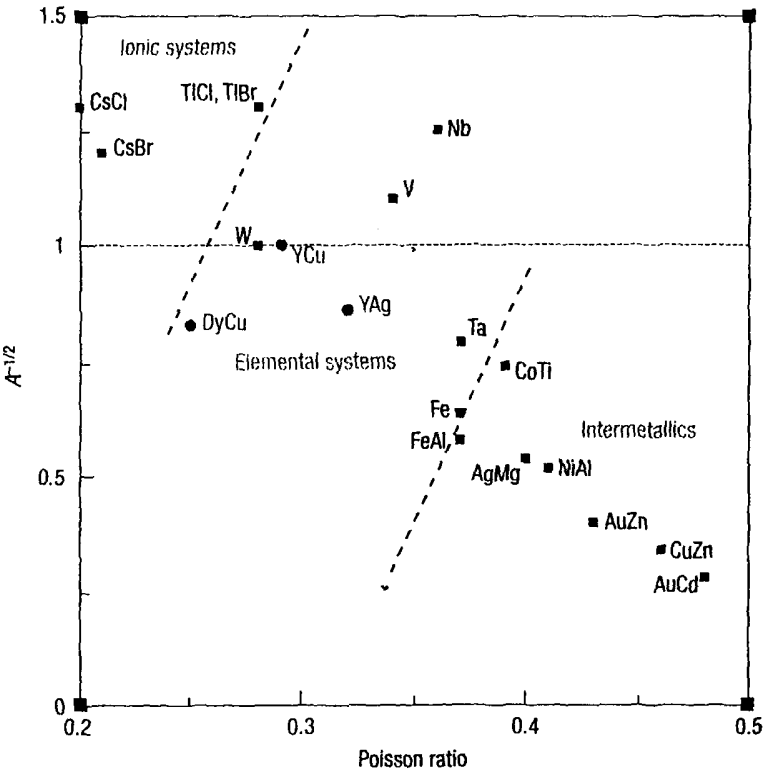
(74) Agent: **TIMMER, Edward, J.**; P.O. Box 770, Richland, MI 49083 (US).

(81) Designated States *(national)*: AE, AG, AL, AM, AT, AU, AZ, BA, BB, BG, BR, BY, BZ, CA, CH, CN, CO, CR, CU, CZ, DE, DK, DM, DZ, EC, EE, ES, FI, GB, GD, GE, GH, GM, HR, HU, ID, IL, IN, IS, JP, KE, KG, KP, KR, KZ, LC, LK, LR, LS, LT, LU, LV, MA, MD, MG, MK, MN, MW, MX, MZ, NI, NO, NZ, OM, PG, PH, PL, PT, RO, RU, SC, SD, SE, SG, SK, SL, SY, TJ, TM, TN, TR, TT, TZ, UA, UG, US, UZ, VC, VN, YU, ZA, ZM, ZW.

(84) Designated States *(regional)*: ARIPO patent (BW, GH, GM, KE, LS, MW, MZ, SD, SL, SZ, TZ, UG, ZM, ZW), Eurasian patent (AM, AZ, BY, KG, KZ, MD, RU, TJ, TM), European patent (AT, BE, BG, CH, CY, CZ, DE, DK, EE, ES, FI, FR, GB, GR, HU, IE, IT, LU, MC, NL, PT, RO, SE,

[Continued on next page]

(54) Title: INTERMETALLIC ARTICLES OF MANUFACTURE HAVING HIGH ROOM TEMPERATURE DUCTILITY



(57) Abstract: Article of manufacture fabricated by plastic deformation of an intermetallic compound comprising R and M, such as an RM intermetallic compound and a higher order compound thereof, having a CsCl-type ordered crystal structure wherein R is one or more rare earth elements and M is one or more non-rare earth metals. The article of manufacture has a tensile elongation of at least about 5% prior to fracture when tensile tested at room temperature in ambient air. The article of manufacture also can be fabricated by plastic deformation of an intermetallic compound comprising a M′M compound and a higher order compound thereof having a CsCl-type ordered crystal structure wherein M′ and M are one or more different non-rare earth metals.

WO 2004/044249 A2

SI, SK, TR), OAPI patent (BF, BJ, CF, CG, CI, CM, GA, GN, GQ, GW, ML, MR, NE, SN, TD, TG).

Published:

— *without international search report and to be republished upon receipt of that report*

For two-letter codes and other abbreviations, refer to the "Guidance Notes on Codes and Abbreviations" appearing at the beginning of each regular issue of the PCT Gazette.

INTERMETALLIC ARTICLES OF MANUFACTURE HAVING HIGH ROOM TEMPERATURE DUCTILITY

This application claims benefits of provisional application Serial No. 60/425,964 filed November 13, 2002.

CONTRACTUAL ORIGIN OF THE INVENTION

The United States Government has rights in this invention pursuant to Contract No. W-7405-Eng-82 between the Department of Energy and Iowa State University.

FIELD OF THE INVENTION

The present invention relates to articles of manufacture made of intermetallic compounds having relatively high ductility at room temperature.

BACKGROUND OF THE INVENTION

Intermetallic compounds, such as TiAl, Ni_3Al, FeAl, $ZrCo_2$ and others, are superior in several ways to conventional metals and alloys. Certain intermetallic compounds are stronger and stiffer at elevated temperature and provide better corrosion resistance than conventional metals and alloys. Some intermetallic compounds also possess exceptional magnetic properties and low densities. However, at room temperature, intermetallic compounds generally are brittle and have low fracture toughness compared to pure metals and solid solution alloys. Hundreds of scientists have worked for more than 50 years to address the problem of room temperature brittleness of intermetallic compounds. Some progress has been made to improve room temperature ductility of the compounds, but reports of high room temperature ductility usually involve some contrivance such as tensile tests conducted in ultra-dry pure oxygen atmospheres, compounds that deviate from stoichiometry, or additions of dopant elements, such as boron, that segregate preferentially to grain boundaries. Reports of stoichiometric binary intermetallic compounds that are ductile under ambient conditions have been noticeably lacking.

SUMMARY OF THE INVENTION

An embodiment of the invention provides an article of manufacture fabricated of an intermetallic compound comprising R and M having a CsCl-type ordered crystal structure wherein R is one or more rare earth elements and M is one or more non-rare earth metals and having high ductility at ambient (room) temperature, such as for purposes of illustration only, at least about 5% tensile elongation prior to fracture when tensile tested at room temperature in ambient air.

One embodiment of the present invention relates to articles of manufacture fabricated of intermetallic compounds selected from the group consisting of an RM compound and a higher order compound thereof having a B2 (CsCl-type) ordered crystal structure wherein R is one or more rare earth elements and M is one or more non-rare earth metals. The articles of manufacture have high ductility at ambient (room) temperature, such as for purposes of illustration only, at least about 5%, preferably about 10% and greater, tensile elongation prior to fracture when tensile tested at room temperature in ambient air. Similarly, the articles of manufacture exhibit high compressive ductilities and fracture toughness at room temperature in ambient air.

Another embodiment of the present invention relates to articles of manufacture fabricated of intermetallic compounds selected from the group consisting of a M'M compound and a higher order compound thereof having a B2 (CsCl-type) ordered crystal structure wherein M' and M are one or more different non-rare earth metals. The articles of manufacture have high ductility at ambient (room) temperature, such as for purposes of illustration only, at least about 5%, preferably about 10% and greater, tensile elongation prior to fracture when tensile tested at room temperature in ambient air. Similarly, the articles of manufacture exhibit high compressive ductilities and fracture toughness at room temperature in ambient air.

Articles of manufacture pursuant to the invention include, but are not limited to, an engine component for an

internal combustion engine of a vehicle including automobiles and trucks, a component for a gas turbine engine, a load-bearing structural component for a vehicle including automobiles, trucks and aircraft, valve, nozzle, separator, a component of a pump, boiler tube, a die for hot or cold pressing, forging or otherwise shaping a metallic or other material, a component of mining or petroleum recovery equipment, a damping component to reduce vibrations, a clad component, a dental component, a component of a medical device, jewelry (particularly black gold formed by one or more oxide layers on the RM material where M = Au), catalyst, getter, diffusion barrier component, an electrical component such as for example a resistor, an electrical contact, an electrical sensor, a battery component, micro-electro-mechanical system (MEMS), a magnetic component such as, for example, a hard or soft magnet, magnetoresistance devices, magnetorestrictors, transducers, hydrogen storage materials, membrane for hydrogen separation and/or purification, coatings, superconductors, metallic mirrors, antibacterial agents, and large neutron absorption cross-section materials containing Sm, Eu, Gd, and/or Dy for nuclear applications, such as control rods, burnable poisons, and shutdown and safety devices for nuclear reactors and nuclear shielding materials.

Still another embodiment involves a method of making an article of manufacture by plastically deforming a body (e.g. an ingot or casting) comprising a ductile intermetallic compound of the type described above.

DESCRIPTION OF THE DRAWINGS

Figure 1 is a diagram of a CsCl-type (B2) crystal structure of an RM intermetallic compound wherein the corners of the unit cell cube are occupied by the M element and the atom in the cube center is the R element. Atom sizes have been reduced for clarity. The {100} and {101} planes and ⟨010⟩ direction for dislocation slip in the YCu intermetallic compound are labeled.

Figure 2 is a stress-strain curve for a polycrystalline YAg tensile specimen tested in air at 22 degrees C. The specimen was ductile in having elongation of 20% at onset of fracture and 27% at final fracture. A plot for a commercially available 3105 Al alloy tested under the same conditions is also shown for comparison.

Figure 3 is a transmission electron micrograph of dislocation structures in a plastically deformed YAg tensile specimen.

Figure 4 is a stress-strain curve for polycrystalline $YCu_{1.005}$ tensile specimen tested in air at 22 degrees C.

Figure 5 is an optical photomicrograph of slip bands on the surface of an YCu single crystal tensile specimen deformed 6% in tension at 22 degrees C. The intersecting lines are slip bands resulting from dislocation motion on the {100} and {101} crystal planes. Scale bar is 0.4 mm high with 0.04 mm graduations.

Figure 6 is a stress-strain curve for polycrystalline DyCu tensile specimen tested in air at 22 degrees C.

Figure 7 is a comparison of the as-received (a) and deformed (b and c) specimens of ErCu compression tested in air at 22 degrees C. Specimen (b) was deformed at 14.1% true strain and specimen at (c) at 20.5% true strain.

Figure 8 shows specimen geometry used for K_{IC} and J_{IC} testing. Dimension W was 24 mm, and the specimen thickness, B, was 10 mm.

Figure 9 shows examples of conventional tensile test results for polycrystalline YAg, YCu, and DyCu. The strain rate was $2x10^{-4}$/second for all specimens.

Figure 10 shows K_{IC} test result for polycrystalline YCu. "COD" is crack opening displacement. The straight line superimposed on the data indicates the 5% secant deviation.

Figure 11 shows load versus load-line-displacement plot for J_{IC} testing of YAg.

Figure 12 shows load versus load-line-displacement plot for J_{IC} testing of DyCu.

Figure 13 shows J-Δa curve determined for YAg as required by the ASTM standard.

Figure 14a shows bright field TEM image and Figure 14b shows conical scan dynamic dark field TEM image of DyCu J_{IC} fracture toughness test specimen. The mean grain size determined by the linear intercept method for this specimen was 0.20 μm.

Figure 15 is a SEM micrograph of fracture surface from a YAg compact tension specimen. Note the absence of intergranular fracture.

Figure 16 is design drawing of the single crystal tensile specimen dimensions produced by electrodischarge machining. The major face of the tensile specimen gauge length is seen here in true shape. The specimen thickness was 1.3 mm.

Figure 17 is a SEM micrograph of the fracture surface from a single crystal $(Tb_{0.88}Dy_{0.12})Zn$ tensile test specimen.

Figure 18 shows stress-strain plots for four YCu single crystal tensile test specimens oriented with the [142] direction parallel to the tensile axis.

Figure 19 is an optical micrograph of slip lines on the $(\bar{8}12)$ plane surface of an YCu tensile test specimen. The tensile axis direction and the slip planes associated with each set of slip lines are labeled. The scale bar is 0.4mm high with 0.04 mm graduations.

Figure 20 shows YCu single crystal compression stress-strain plots. Compression of the specimen labeled "1" was halted shortly after the first serrations in the stress-strain plot appeared. Specimen #1 showed no slip lines on the polished surfaces. Compression of the specimen labeled "2" was continued well beyond the first serrations in the stress-strain plot, and this specimen underwent extensive surface distortion, as shown in Figure 21. The serrations in the curves are thought to result from a stress-induced transformation to the B27 structure.

Figure 21 is a SEM micrograph of YCu compression test specimen #2 showing topographic displacement of the initially flat {100} surfaces. The feature running vertically through the center of the micrograph is the corner of the specimen where two specimen faces meet at right angles. The compression axis was parallel to this corner. Prior to the compression test, the specimen faces were perpendicular {100} planes that had been polished flat. The distortion of these surfaces is thought to be the result of a stress-induced transformation from the B2 crystal structure to the B27 crystal structure.

Figure 22 shows a comparison of the anisotropy factor, $A^{-1/2}$, versus the Poisson ratio for YAg, YCu, and DyCu as well as for body-centered cubic (bcc) transition metals, ionic compounds, and non-RM intermetallic compounds for comparison.

DETAILED DESCRIPTION OF THE INVENTION

One embodiment of the present invention involves articles of manufacture fabricated of ordered intermetallic compounds comprising R and M having a B2 (CsCl-type) ordered crystal

structure wherein R is one or more rare earth elements and M is one or more non-rare earth metals, preferably one or more late transition metals or early p-group metals from Groups I, II, or III) of the Periodic Table. The intermetallic compound can be selected from the group consisting of an RM compound and a higher order RM compound thereof having the B2 (CsCl-type) ordered crystal structure where a higher order compound means that instead of a single rare earth element, R, two, three, four or more different rare earth elements are taken in various proportions; and instead of a single non-rare earth element M, two, three, four, or more different non-rare earth elements are taken in different proportions thus forming a (R_1, R_2, R_3, . . .) (M_1, M_2, M_3, . . .) compound, i.e. a first order compound is a binary one (e.g. RM), a second order compound has three components [e.g. $R(M_1,M_2)$] or $(R_1,R_2)M$, a third order compound has four components [e.g. $(R_1,R_2)(M_1,M_2)$] and so forth. An illustrative B2 (CsCl-type) ordered crystal structure is illustrated in Figure 1 wherein the corners of the unit cell cube are occupied by the M element and the atom in the cube center is the R element.

The R element is selected from one or more rare earth elements. The R element is selected from the group consisting of Sc, Y, La, Ce, Pr, Nd, Pm, Sm, Eu, Gd, Tb, Dy, Ho, Er, Tm, Yb, and Lu and combinations thereof. The M element is selected from one or more non-rare earth metals and preferably is selected from the group consisting of Mg, Al, Co, Ni, Cu, Zn, Ru, Rh, Pd, Ag, Cd, In, Ir, Pt, Au, Hg, and Tl and combinations thereof. For purposes of illustration, Table 1 lists the binary RM CsCl-type intermetallic compounds formed by rare earth elements and non-rare earth metals. The M element also can be selected from a metal or a non-metal not mentioned above (e.g. Li, B, C, Si, P, Ga, Ge, etc.) to modify a particular property of the article of manufacture for a particular application and whose concentration is limited to the maximum solid solubility of that metal in the compound such that the compound retains the B2 (CsCl-type) ordered crystal structure.

Articles of manufacture are made of binary RM compounds as well as ternary RM compounds, such as $(R_xR'_{1-x})M$ and $R(M_xM'_{1-x})$, and higher order RM compounds, such as $(R_xR'_{1-x})(M_xM'_{1-x})$ even including $(R,R'...R^n)(M,M'...M^n)$, where the prime designates a different R or M element from the non-prime R or M and where n can be 3, 4 or more and designates a different R or M element from the other R or M elements of the compound.

Table 1. Binary Rare Earth Intermetallic Compounds with the CsCl-type Structure

Non-Rare Earth Metal	Rare Earth Metals
Mg	Sc, Y, La, Ce, Pr, Nd, Sm, Gd, Tb, Dy, Ho, Er, Tm and Lu
Al	Sc[a]
Co	Sc
Ni	Sc
Cu	Sc, Y, Sm,[a] Eu, Gd, Tb, Dy, Ho, Er, Tm and Lu
Zn	Sc, Y, La, Ce, Pr, Nd, Sm, Eu, Gd, Tb, Dy, Ho, Er, Tm, Yb and Lu
Ru	Sc, Yb, Lu
Rh	Sc, Y, Sm, Gd, Tb, Dy, Ho, Er, Tm, Yb and Lu
Pd	Sc, Dy, Ho, Er,[a] Tm, Yb and Lu
Ag	Sc, Y, La, Ce,[a] Pr, Nd, Sm, Gd, Tb, Dy, Ho, Er, Tm, Yb[a] and Lu
Cd	Sc, Y, La, Ce, Pr, Nd, Sm, Gd, Tb, Dy, Ho, Er, Tm, Yb and Lu
In	Y, La, Pr, Sm, Gd[a], Dy, Ho, Er, Tm and Yb
Ir	Sc, Y, Ho, Er, Tm, Yb and Lu
Pt	Sc
Au	Sc, Y, Pr[a], Nd[a], Sm[a], Gd[a], Tb[a], Dy[a], Ho[a], Er[a], Tm[a], Yb[a] and Lu
Hg	Sc, Y, La, Ce, Pr, Nd, Sm, Eu, Gd, Tb, Dy, Ho, Er, Tm, Yb and Lu
Tl	Y, La, Ce, Pr, Nd, Sm, Eu, Gd, Tb, Dy, Ho, Er, Tm and Yb

[a]Polymorphic: CsCl-type and CrB-type or FeB-type

For purposes of illustration and not limitation, Table 2 lists binary intermetallic compounds pursuant to another embodiment of the invention, which compounds have the CsCl-type crystal structure and which do not have a rare earth element as a component. Such compounds are selected from the group consisting of a M'M compound and a higher order M'M compound thereof having a B2 (CsCl-type) ordered crystal structure wherein M is one or more different non-rare earth metals. The mechanical behavior of some of these compounds may exhibit high ductility in tension and compression at room (ambient) temperature in ambient air. Most likely ductile candidate compounds include, but are not limited to HgMg, HgSr, LiPb, MgTl, and PuRu.

Table 2. Binary Non-Rare Earth Intermetallic Compounds with the CsCl-type Structure

AgLi
AgZn
AlAu
AlIr
AlMn
AlOs
AlPd
AlPt
AlRe
AlRh
AuCd
AuCs
AuLi
AuMg
AuMn
AuRb
AuTi
AuZn
BaCd
BaHg
BaZn
BeCo
BeCu
BeNi
BePd
BeRh
BeTi
BiTh
BiTl
CaCd
CaHg
CaIn
CaPd
CaTl
CdSr
CoGa
CoHf
CoTi
CoZr
Cu-Pd
FeRh
FeTi
FeV
GaIr
GaNi
GaRh
GaRu
HfOs
HfPt
HfRh
HfRu
HfTc
HgLi
HgMg
HgMn
HgSr
HgTl
InNi
InPd
InRh
InSb
IrMn
IrTi
IrZr
LiPb
LiTl
MgPd
MgRh
MgTl
MnNi
MnPd
MnPt
MnRh
MnV
MnZn
NbRu
NiTi
NiZn
OsSi
OsTi
OsV
OsZr
PdTi
PtTi
PtZr
PuRu
ReTi
RhSi
RhZr
RuSi
RuTi
Ru-V
RuZr
SrTl
TaTc
TcTi
TcV
TeTh
TiZn
ZnZr

The articles of manufacture have high ductility in tension and compression at room (ambient) temperature in ambient air. For example, the articles of manufacture preferably exhibit at least about 5%, more preferably about 10% and greater, tensile elongation prior to fracture when tensile tested at room (ambient) temperature in ambient air pursuant to ASTM test E8-82 described in the publication Annual Book of ASTM Standards, published by American Society for Testing and Materials, 1985, V. 301, West Conshohocken, PA, USA, which is incorporated herein by reference with respect to the test procedure. The articles of manufacture exhibit similar high compressive ductilities and fracture toughness at room (ambient) temperature in ambient air.

The invention will be described below with respect to articles made from intermetallic compounds that are so-called line compounds (relative to a phase diagram of R and M) that do not deviate from ideal stoichiometry (e.g. 1:1 stoichiometry for RM compounds) as a result of being made of high purity R and M starting materials. The invention is not limited to such stoichiometric, so-called line RM or M'M intermetallic compounds and envisions articles made of near-stoichiometric or off-stoichiometric intermetallic compounds as a result of the presence in the intermetallic compound of incidental impurities, such as for example interstitial impurities including H, B, C, N, O, and F and/or as a result of loss of the R and/or M (or M' and/or M)constituent during melting and other manufacturing steps of the compound so long as the article of manufacture exhibits a high ductility at ambient (room) temperature such as at least 5%, preferably 10% and greater, tensile elongation prior to fracture when tensile tested at room temperature in ambient air pursuant to ASTM test E8-82 and has an ordered CsCl B2 crystal structure. The invention also envisions addition of one or more constituents other than R and M (or M' and M) to the intermetallic compound (e.g. ternary, quaternary, etc. compounds) so long as the

article of manufacture exhibits a high ductility at ambient (room) temperature such as at least 5%, preferably 10% and greater, tensile elongation prior to fracture when tensile tested at room temperature in ambient air pursuant to ASTM test E8-82 and has an ordered CsCl B2 crystal structure.

For purposes of illustration, specimens fabricated of the following binary and ternary RM intermetallic compounds were tested for ductility in a simple hammer and anvil test (if specimen deformed and did not shatter, it was ductile) conducted at room temperature in ambient air: YAg, YCu, CeAg, DyCu, ErAg, ErAu, ErCu, ErIr, HoCu, NdAg, $(Tb_{0.88}Dy_{0.12})Zn$, YIn, and YRh. Of these specimens, all were ductile with the exception of $(Tb_{0.88}Dy_{0.12})Zn$. The specimens for ductility tests were prepared by arc-melting and solidifying the melted material on a water-cooled hearth to produce a disk-like shape with a rounded top and flat bottom and a diameter of about 10 mm.

Other standard metallurgical processing procedures may also be used to prepare these compounds - such as induction melting, or heating in a resistance furnace using an appropriate crucible under an inert gas or vacuum. For those B2 compounds which contain a volatile component, such as R = Sm, Eu, Tm, and Tb, or M = Mg. Zn, Cd, Hg, and Tl but not limited to these elements, a sealed crucible (such as Ti, V, Zr, Nb, Mo, Hf, Ta, W, BN, refractory oxide materials, etc.) may need to manufacture the B2 intermetallic compound without the loss of a portion of the high vapor pressure component. For those RM and M´M (and higher order compounds) which are polymorphic (including but not limited to ScAl, SmCu, ErPd, CeAg, YbAg, GdIn, RAu, LiPb) rapid solidification techniqures, such as splat cooling, melt spinning, roller quenching, liquid quenching, vapor quenching, sputtering, flash evaporation, etc., may be necessary to retain the high temperature B2 phase.

Articles of manufacture fabricated of ScM intermetallic compounds, such as ScMg, ScAl, ScCo, ScNi, ScCu, ScZn, ScRu,

ScRh, ScPd, ScAg, ScCd, ScIr, ScPt, ScAu, ScHg and ternary alloys such as $Sc(M_xM'_{1-x})$ and $(Sc_xR'_{1-x})M$ have considerable interest since most of these compounds melt congruently above 1000 degrees C, making them attractive for fabrication into articles of manufacture for use at high temperatures. For example, all of these compounds melt congruently, except ScCo which melts incongruently. By way of further example, ScAl melts at 1300 degrees C; ScCo melts at 1050 degrees C; ScNi melts at about 1300 degrees C; ScCu melts at 1125 degrees C; ScRu melts at 2200 degrees C; ScPd melts at 1600 degrees C; ScAg melts at 1230 degrees C; ScPt melts at about 2200 degrees C. Considering the current cost associated with the non-Sc element (i.e. M element), articles of manufacture fabricated of ScAl, ScNi, ScCu, ScRu, and ScAg appear to be candidates for high temperature service applications. An article of manufacture fabricated of ScAl is attractive for aerospace applications because of its low density (about 3.0 g/cm^3 for ScAl). Articles of manufacture fabricated of ScRu and ScPt are attractive for high temperature service applications as a result of the extremely high melting points (about 2200 degrees C for ScRu and ScPt). An article of manufacture fabricated of LuRu having a melting point of 2200 degrees C is also attractive for high temperature service applications as a result of the extremely high melting point of LuRu.

The articles of manufacture pursuant to the invention thus may be used over wide ranges of temperatures depending upon the particular RM or M'M intermetallic compound from which the article is fabricated. From an engineering perspective, such articles of manufacture can provide improved high temperature strength, stiffness, and oxidation resistance, yet they would be deformable at room temperature and resist brittle fracture as a result of their high ductility.

Articles of manufacture pursuant to the invention can be fabricated of the ordered RM intermetallic compounds by melting the pure R element(s) and pure M element(s) together to form a

melt and casting the melt into a mold or die to form a shaped polycrystalline or single crystal article of manufacture. The same is true of the M'M compounds. For purposes of illustration and not limitation, melting can be conducted using conventional arc-melting procedures under vacuum or under inert gas atmosphere in crucibles comprising any suitable refractory, ceramic or other material that is not adversely reactive with the melt. The melt can be conventionally cast into a mold, which may comprise a metal mold or die, a refractory mold, a ceramic mold, or any other suitable mold. Ingots or other bodies of the RM or M'M intermetallic compound can be made and forged, rolled, or otherwise plastically hot or cold worked or deformed to a suitable shape of an article of manufacture as a result of the ductility of the RM or M'M material. Powders of the RM or M'M intermetallic compound can be made by standard techniques, such as including but not limited to gas atomization and plasma rotating electrode processes and consolidated by conventional processes such as hot or cold isostatic compression, pressing and other powder consolidation processes into a suitable shape of an article of manufacture as a result of the ductility of the RM or M'M material.

The following EXAMPLES are offered to further illustrate and not limit the invention.

EXAMPLES

Example 1): Polycrystalline specimens of equiatomic YAg were produced by arc-melting the pure elements on a water-cooled copper hearth in an inert gas (Ar) atmosphere to form an ingot in the shape of a finger or disk depending on the shape of the mold in the copper hearth. The specimens comprised 50 atomic % Y and 50 atomic % Ag. X-ray diffraction and metallography studies of the cast specimens confirmed that they were single-phase with fully ordered CsCl-type crystal structure. The cast specimens were annealed for 86 kiloseconds at 800 degrees C and machined into cylindrical tensile test specimens, which were tensile tested to failure in room temperature air at a strain

rate of $2x10^{-4}$/second.

Figure 2 is a representative stress-strain curve for the machined YAg specimens. Also shown in Figure 2 is a stress-strain curve for a commercially available aluminum alloy (3105) widely used for gutters, downspouts, window frames and siding. The machined YAg specimen unexpectedly and surprisingly exhibited a large tensile elongation (more than 20% increase in length prior to fracture) comparable to that exhibited by the Al 3105 alloy. Figure 3 is a transmission electron micrograph of dislocation structures in a plastically deformed (27% elongation) YAg specimen.

Example 2): Polycrystalline specimens of nearly equiatomic $YCu_{1.005}$ were produced by arc-melting the pure elements on a water-cooled copper hearth in an inert gas (Ar) atmosphere to form an ingot in the shape of a finger or disk depending on the shape of the mold in the copper hearth. This specimen was made with a starting composition of $Y_{1.000}Cu_{1.005}$ because small losses of Cu occur during arc-melting through vaporization, and this starting composition yields a final cast specimen that is close to the perfect 1:1 stoichiometry. X-ray diffraction and metallography studies of the cast specimens confirmed that they were single-phase with fully ordered CsCl-type crystal structure. The cast specimens were annealed for 36 kiloseconds at 700 degrees C and machined into cylindrical tensile test specimens, which were tensile tested to failure in room temperature air at a strain rate of $2x10^{-4}$/second.

Figure 4 is a representative stress-strain curve for the machined YCu specimens. The machined YCu specimens unexpectedly and surprisingly exhibited a large tensile elongation (more than 12% increase in length prior to fracture).

Example 3): Eight single crystal YCu tensile specimens were produced by the well known Bridgman (power-down) technique where a YCu melt in a mold or crucible is directionally

solidified therein by gradually reducing induction heating power along the length of the melt to form a single crystal body. The tensile specimens were machined from the single crystal cast bodies and polished by 0.25 micron diamond abrasive in an oil suspension. All eight tensile specimens had a tensile axis of direction [142] with polished surfaces corresponding to the (-812) and (-2 6 -11) planes. The specimens were pulled in tension at room temperature (22 degrees C) in air at a strain rate of $1x10^{-4}$/second. The specimens exhibited a yield stress of 45 MPa and fractured at 6% to 8% elongation at a stress of 75 to 90 MPa.

Figure 5 is an optical photomicrograph of slip bands on the surface of an YCu single crystal test specimen deformed 6% in tension at 22 degrees C. The intersecting lines are slip bands resulting from dislocation motion on the {100} and {101} crystal planes. On both slip planes, the slip direction was ⟨010⟩.

Example 4): Polycrystalline specimens of equiatomic DyCu were produced by arc-melting the pure elements on a water-cooled copper hearth in an inert gas (Ar) atmosphere to form an ingot in the shape of a finger or disk depending on the shape of the mold in the copper hearth. The specimens comprised 50 atomic % Dy and 50 atomic % Cu. X-ray diffraction and metallography studies of the cast specimens confirmed that they were single-phase with fully ordered CsCl-type crystal structure. The cast specimens were annealed for 43 kiloseconds at 600 degrees C and machined into cylindrical tensile test specimens, which were tensile tested to failure in room temperature air at a strain rate of $2x10^{-4}$/second.

Figure 6 is a representative stress-strain curve for the machined DyCu specimens. The machined DyCu specimen unexpectedly and surprisingly exhibited a large tensile elongation (more than 14% increase in length prior to fracture).

Example 5): Polycrystalline specimens of equiatomic ErCu were produced by arc-melting the pure elements on a water-cooled copper hearth in an inert gas atmosphere (Ar) to form an ingot in the shape of a finger or disk depending on the shape of the mold in the copper hearth. The specimens comprised 50 atomic % Er and 50 atomic % Cu. X-ray diffraction and metallography studies of the cast specimens confirmed that they were single-phase with fully ordered CsCl-type crystal structure. The cast specimens were machined into cylindrical compressive test specimens, which were subjected in room temperature air to the true strains of 10.4%, 14.1%, and 20.5% at a strain rate of 2.8×10^{-4}/second.

Figure 7 shows the comparison of the deformed specimens at 14.1% (b) and 20.5% (c) true strains with the undeformed specimen (a). The most remarkable feature is the fact that although ErCu was deformed to greater than 20% true strain (c), no macroscopic cracks were generated. A summary of the mechanical properties of the deformed ErCu is given in Table 3.

Table 3

Proportional limit -78 plus or minus 7.5 MPa
Yield point - 187 plus or minus 19.7 MPa
True strength (at 10% true strain) - 401.7 plus or minus 16.8 MPa
Room temperature ductility - greater than 20%

Example 6): Fracture toughness is an important mechanical property when assessing possible engineering applications for intermetallic compounds. However, there are relatively few reports in the literature of intermetallics that have been measured by the ASTM standard tests for plane strain fracture toughness (K_{IC}) or material toughness near the onset of crack extension from a preexisting fatigue crack (J_{IC}). The few

measurements that have been reported have been taken from composite materials comprised of mixed ductile and intermetallic phases or from intermetallic compounds that are off-stoichiometry. Although considerable attention has been devoted to the general topic of fracture toughness of intermetallics, toughness is usually estimated by the Palmqvist method or by Charpy testing rather than the more time consuming ASTM standard tests (i.e. ASTM E 399-90 or ASTM E 813-89) used on conventional metals. The ASTM tests are poorly suited to measurement of brittle materials, and most intermetallics have low tensile ductility in air at ambient temperature.

The room temperature fracture toughness was measured for YCu, DyCu, and YAg specimens. Standard tensile tests indicated that YCu was the least ductile of these three intermetallics (11% elongation at failure); DyCu had an intermediate ductility (16% elongation at failure); while YAg was the most ductile (20% elongation at failure). The K_{IC} value was determined directly for YCu using ASTM test method E 399-90; J_{IC} values were measured using ASTM test method E 813-89 for DyCu and YAg, and these J_{IC} values were converted to K_{IC} values. The K_{IC} values were found to be 12.0 $MPa\sqrt{m}$ for YCu, 25.5 $MPa\sqrt{m}$ for DyCu, and 19.1 $MPa\sqrt{m}$ for YAg. These vales are high for fully ordered, stoichiometric intermetallic compounds tested in room air of normal humidity.

Arc-melted buttons of YCu, DyCu, and YAg were prepared from high-purity Dy (99.94 wt.%), Y (99.94 wt.%), Cu (99.99 wt.%), and Ag (99.994 wt.%). The top of each button was milled slightly to produce a flat for rolling, and each button was encapsulated in a stainless steel can that was welded shut inside a dry Ar atmosphere glove box. The canned buttons were then hot rolled at 700 C to reduce specimen thickness from 16 mm to 13 mm. After rolling the stainless steel cans were removed, and fracture toughness compact tension specimens (CT)

were cut from the rolled buttons by electrodischarge machining (EDM) to the dimensions shown in Figure 8. The specimens were extracted from the T-L position (i.e. the specimen is machined to align the crack plane parallel to the rolling direction). For both K_{IC} and J_{IC} testing, the finished specimens had overall dimensions of 30 mm x 29 mm x 10 mm, with W equal to 24 mm and thickness (B) equal to 10 mm. After machining, specimens were wet polished to 800-grit finish, followed by a final polishing step using 1 μm diamond paste.

EDM line cutting was then used to produce a notch with root radius, r, equal to 0.125 mm. Samples were then fatigue precracked using a servo-hydraulic MTS machine in room air in cyclic loading using a sinusoidal wave of 5 Hz. During the fatigue pre-cracking a nominal stress intensity range was 5-10 MPa with an R ratio of 0.1. The final fatigue crack lengths were in the range of a/W ~0.45-0.55. Fatigue crack advance was monitored by a traveling optical microscope.

Fracture toughness (K_{IC}) was determined following the procedures of the ASTM test method E 399-90 at ambient temperature using an Instron screw-driven mechanical testing machine. The tests were performed under displacement control with a constant cross-head movement rate of 0.02 mm/min. The load-crack opening displacement (COD) was monitored and recorded through a clip gauge attached to the front face of the specimen.

For DyCu and YAg, large specimen thicknesses are required in order to meet the validity criterion of ASTM test method E 399-90, so the fracture toughness for these two materials was obtained using the J_{IC} testing technique following ASTM Standard test method E813-89. The E813-89 protocol provides an alternative means to determine the K_{IC} value with a smaller required specimen thickness. Prior to J_{IC} testing, the precracked samples with a/W ratio of 0.5-0.55 were 15% side grooved by EDM line cutting along the front of the pre-crack to confine crack growth to the same plane as that of pre-

cracking, as described in the ASTM standard. The J_{IC} fracture toughness test procedure was the single specimen technique with partial unloading according to ASTM test method E 813-89. The specimen was first pulled to determine the initial crack length, and then loaded by a repeated loading and partial-unloading scheme. The tests were performed in air under displacement control, with the displacement rate of 0.002 mm/s as recommended in the standard. A clip gauge was used to detect front-face crack opening displacement, and this value was later converted to load-line displacement for the J_{IC} calculation.

After the fracture toughness test was completed, SEM micrographs were taken from the fracture surfaces. In addition, coupons about 0.5 mm thick were cut from a region of the DyCu J_{IC} test specimen distant from the crack. These coupons were used to make specimens for transmission electron microscopy (TEM) study. TEM foils were prepared by mechanical dimpling and then by Ar ion beam milling to perforation. A grain size determination was made using the linear intercept method from bright field and conical scan dynamic dark field micrographs obtained with a Philips CM30 300kV TEM.

Ordinary round tensile test specimens with gauge sections 2.4mm in diameter and 9.6mm long were prepared for conventional tensile testing using the same purity elements as were used for the CT specimens. These alloys were initially prepared as arc-melted buttons. The buttons were then placed inside a Ta crucible and melted in vacuum with inverted Ta tubes (3mm inside diameter). The molten intermetallic was vacuum aspirated into the Ta tubes, and this assembly was cooled and removed from the furnace. The 3mm Ta tubes containing solid intermetallic were then cut away from the left-over intermetallic that was not aspirated into the tubes. The Ta tubes filled with intermetallic were cold swaged to a 10.9% reduction in area and annealed in He at 500 C for one hour. The Ta sleeves were machined from the specimens and

tensile test specimens (proportioned as per ASTM Standard E8) were cut on an ordinary lathe. Tensile testing was performed at a strain rate of $2x10^{-4}$/second to failure.

The results from three of the conventional tensile tests are shown in Figure 9. All three intermetallics show higher ductility (~11 to 20% elongation) than would normally be expected for polycrystalline, stoichiometric, fully ordered intermetallic tensile specimens tested in room air. The YAg consistently displayed the highest ductility of the three compositions. The 0.2% offset yield strengths of the tensile test specimens of all three compositions varied considerably from one specimen to the next. Examination of the fracture surfaces of these specimens showed that some had pre-existing cracks, which would, of course, lower the specimen's apparent strength. For those specimens whose fracture surfaces showed no evidence of pre-existing cracks, the YCu 0.2% offset yield strengths were considerably higher than those of the YAg and DyCu.

The K_{IC} testing result for YCu is shown in Figure 10. The critical Load P_Q was obtained using the 5% secant deviation technique specified by the standard. From the P_Q value, the K_Q value was determined using the standard stress intensity factor calibration function for compact tension specimens as described in the standard:

$$K_Q = \frac{P_Q}{BW^{1/2}} f(a/W) \qquad (1)$$

where P_Q is the load at fracture instability, B is the specimen thickness, W is the specimen width, a is the notch plus crack length, and f(a/W) is a dimensionless function:

$$f(a/W) = \frac{[2+(a/W)][0.866+4.64(a/W)-13.32(a/W)^2+14.72(a/W)^3-5.6(a/W)^4]}{[1-(a/W)]^{3/2}} \qquad (2)$$

Using equation (3) given below, the K_Q is obtained as 12.0 $MPa\sqrt{m}$. The value of P_{max}/P_Q is about 1.1, satisfying the requirement for a valid plane strain K_{IC} test for YCu. On the other hand, the P_{max}/P_Q values determined for DyCu were significantly larger than 1.1, which indicated that a valid K_{IC} test could not be made to determine the plane strain fracture toughness of DyCu with the available specimen thickness of 10 mm.

According to ASTM test method E 399-90, a state of plane strain is achieved when the sample thickness is greater than $2.5(K_{IC}/\sigma_y)^2$, i.e., the thickness is significantly larger than the plastic or damage zone size of $r_y \sim 1/2\pi(Kc/\sigma_y)^2$. For YCu, which has a yield strength of ~200 MPa, this requires sample thickness of approximately 10 mm. However, DyCu and YAg have lower yield strengths than YCu, and if their K_{IC} values are similar to those of YCu, the required thickness for these materials would be more than 20 mm. Arc melting buttons to such large thicknesses was not feasible, so J_{IC} tests were performed for DyCu and YAg.

The J_{IC} tests of DyCu and YAg were performed using the single specimen technique; three DyCu specimens and two YAg specimens were tested. Typical curves of load versus load-line displacement for YAg and DyCu are presented in Figures 11 and 12 respectively. The load-line-displacement, V_{LL}, in each figure was converted from the COD value, measured from the front face attached clip gauge. For each partial unloading in Figures 11 and 12, the actual J-integral and the corresponding crack advance Δa were calculated. The J-integral for each step was calculated from the plastic area of the load vs. load-line-displacement curve up to the maximum load point according to the following equation:

$$J = \frac{2U}{B_0(W-a)}, \qquad (3)$$

and Δa was deduced from the compliance variation of the current unloading step, using the formula in the standard. The R curve was thus obtained in accordance with the data reduction method described in the standard, and the obtained curve is shown in Figure 13, where the YAg behavior is displayed. The R curve was then fitted using polynomial approximation. The $J_{0.2}$-value, defined as the ordinate of the intersection of the R curve with a parallel to the blunting line at Δa=0.2 mm, was obtained as the J_{IC} value for the tested material, as described in the standard. The mean estimated value of J_{IC} was ~3850 J/m^2 for YAg and ~6890 J/m^2 for DyCu. The two J_{IC} values for YAg and the three values for DyCu are given in Table 1.

The resulting K_{IC} was then calculated using:

$$J_{Ic} = \frac{1-\nu^2}{E} K_{Ic}^2 \qquad (4)$$

The calculated K_{IC} is 19.1 MPa$\sqrt{m}$ for YAg and 25.5 MPa$\sqrt{m}$ for DyCu, where values for Poisson's ratio (ν=0.303) and elastic modulus (E=85.6 GPa) were determined from acoustic ultrasound measurements performed on single crystals. The K_{IC} and J_{IC} values determined in this example are summarized in the Table 4 below.

Table 4 J_{IC} and K_{IC} values of RM intermetallics. K_{IC} values for YAg and DyCu were calculated from the J_{IC} values.

Material (no. of test specimens)	J_{IC} (J/m^2)	K_{IC} ($MPa\sqrt{m}$)
YCu (1)	not measured	12.0
YAg (2)	3810	18.9
	3890	19.2
	mean = 3850	mean =19.1
DyCu (3)	5670	23.2
	7900	27.6
	7100	25.8
	mean = 6890	mean= 25.5

The large ductility and high fracture toughness of these B2 compounds is surprising. Research on other intermetallics has led to the general conclusion that high ductility and high fracture toughness are most likely to occur in compounds with a low ordering energy (e.g. B2 CuZn), compounds that are off-stoichiometry (e.g. Fe-35%Al), or compounds tested in a dry oxygen atmosphere or in vacuum. None of these factors exists in the RM compounds examined in this example. The ordering energies of YCu, DyCu, and YAg are believed to be high; these specimens were fully ordered and exactly stoichiometric, and they were tested in ordinary room air. The fracture toughness values for the DyCu specimens are comparable to those of commercial aircraft aluminum alloys. For comparison, K_{IC} is only 5 to 6 $MPa\sqrt{m}$ for NiAl B2 intermetallic compounds.

Figure 14a and 14b show the mean grain size in DyCu J_{IC} specimen was quite small, e.g. 0.2 μm. Fine grain size tends to increase fracture toughness by minimizing dislocation pile-up stresses. It is significant to note that the CT specimen fracture surfaces shown in Figure 15 display no evidence of

intergranular fracture.

Example 7): Further single crystal specimens of YCu with the B2-type crystal structure were tested in tension and in compression, and isostructural single crystal specimens of B2 $(Tb_{0.88}Dy_{0.12})Zn$ were tested in tension. The YCu tensile specimens elongated 6% to 8% before fracture. The active slip systems in YCu in tension were found to be {100}<010> (τ_{CRSS} = 17 MPa) and {110}<010> (τ_{CRSS} = 18 MPa). Specimens of single crystal YCu were compression tested with the <100> direction as the compression axis, an orientation that puts no resolved shear stress on either the {100}<010> or the {110}<010>. These compression tests resulted in high yield stresses followed by what is believed to be a stress-induced transformation to another crystallographic structure of YCu, the B27-type crystal structure. All specimens of $(Tb_{0.88}Dy_{0.12})Zn$ failed by brittle fracture.

For example, single crystals of YCu and $(Tb_{0.88}Dy_{0.12})Zn$ were grown in sealed Ta crucibles by the conventional Bridgman (power down) technique. The rare earth metals used in this study were obtained from the Department of Energy, Ames Laboratory Materials Preparation Center, Ames, Iowa, and they were 99.9 at.% pure. The Cu and Zn (both 99.99% purity) were purchased from Copper and Brass Sales, and Cerac, respectively. For YCu the starting ingots for single crystal growth were prepared by arc-melting appropriate quantities of Y and Cu under an Ar atmosphere. The buttons were remelted several times, turning the button between melts. Finally, the alloy was drop cast into a Cu chill cast mold to ensure compositional homogeneity throughout the ingot. The YCu was placed inside the Ta Bridgman crucible and then sealed by electron beam welding a Ta lid onto the crucible.

Appropriate quantities of Tb, Dy, and Zn were co-melted in a sealed Ta crucible under slightly less than 100 kPa of

Ar. This crucible was then heated to 1475 K, cooled, and inverted before re-heating. This sequence of melting was repeated twice before crystal growth began to provide a complete and homogeneous mixing of the elemental constituents.

The crucibles containing the alloys were heated under a pressure of 1.3×10^{-4} Pa up to 1075 K to degas H from the crucible. The chamber was then backfilled to a pressure of 275 kPa with high purity Ar. The ingot was then further heated to the growth temperature and held for 3.6 ks (1 hr) to allow thorough mixing before withdrawing the sample from the heat zone at a rate of 1.1 μm/s. X-ray diffraction analysis confirmed the crystals' single-phase, fully ordered B2 structure.

The single crystals' orientations were determined using Laue X-ray back reflection analysis, and the specimens were cut into tensile specimens (Figure 16) and compression specimens by electro-discharge machining. Following machining the orientations of the specimens were again checked by Laue X-ray back reflection analysis, and the sides of the specimens' gauge length were polished using 1 μm diamond paste in an oil suspension.

Four single crystal tensile specimens of YCu were tested, all having the [142] direction parallel to the tensile axis. The major faces of these specimens were $(\bar{8}12)$ planes, and the minor faces were $(\bar{2}6\bar{1}\bar{1})$ planes. Eight single crystal tensile specimens of $(Tb_{0.88}Dy_{0.12})Zn$ were produced; four had the [100] direction parallel to the tensile axis; two had the [211] direction parallel to the tensile axis; and two had the [111] direction parallel to the tensile axis. Two compression specimens of YCu were produced. Each was a parallepiped 10 mm high with a square cross section 3 mm on a side. These compression specimens were oriented with the 10mm dimension and the [001] direction parallel to the compression axis and with {100} planes as the polished specimen faces.

Extensometers were not used on the specimens due to their small sizes; the strain values reported are based on crosshead position read-outs. Since this is an inherently less accurate method of strain determination, strain values reported here should be considered approximate.

Tensile tests were conducted to fracture at room temperature in normal humidity air. The strain rate for all tensile tests and compression tests was $1x10^{-4}$/second. Compression tests were conducted at room temperature in air to a maximum of 3.3 % strain and then halted. Slip lines on the specimen surfaces were photographed using both optical and scanning electron microscopy.

7.1 $(Tb_{0.88}Dy_{0.12})Zn$ Tensile Tests

All eight specimens of $(Tb_{0.88}Dy_{0.12})Zn$ failed by brittle fracture. The tensile strengths measured in these tests are presented in Table 5 below. Some of the specimens had fracture strengths exceeding 200 MPa, which is relatively high for a single crystal. No slip lines were observed on the specimen faces. These specimens all showed cleavage fracture surfaces (Figure 17). Gas fusion analysis of the $(Tb_{0.88}Dy_{0.12})Zn$ crystals indicated that the H content was relatively low, ranging from 30 to 45 wt. ppm. These H levels are essentially the same as those in the more ductile YCu specimens tested in this study, which suggests that the $(Tb_{0.88}Dy_{0.12})Zn$ specimens were not embrittled by H, but are inherently brittle.

7.2 YCu Tensile Tests

All four single crystal tensile specimens of YCu displayed significant ductility. Elongations at maximum load ranged from 6% to 8%; final fracture occurred at 7.6% to 9.5% elongation. Stress-strain plots for these specimens are shown in Figure 18. All fractures occurred in the specimen gauge section. The tensile strengths measured in these tests are presented in Table 6 below. The slip lines observed on the specimen faces are shown in Figure 19; these slip lines had the same orientations on all four specimens.

7.3 YCu Compression Tests

Compression tests were performed on two single crystal specimens of YCu machined to orient the [001] direction parallel to the compression axis. This orientation produces no resolved shear stress on <100> slip directions, and for many B2 compounds (e.g. NiAl) this is a "hard" orientation because it stymies slip in the <100> direction where slip often occurs most easily. As Figure 20 shows, the compression tests on YCu with this orientation resulted in yield stresses as high as 300 MPa followed by serrations in the stress-strain plot from discontinuous yielding. Each stress drop shown on Figure 20 was accompanied by the distinctive sound that often accompanies twinning in a tensile specimen.

The serrations from discontinuous yielding on the stress-strain plots and the acoustic reports could be caused by twinning, kink band formation, or by a stress-induced transformation to another crystal structure. The YCu B2 crystal structure has been reported as the equilibrium structure at room temperature; however, at low temperature (~140 K) the B2 structure transforms to the orthorhombic B27 (FeB) structure.

After the compression testing, X-ray diffraction (XRD) analysis was performed on the compression specimen labeled "2" in Figure 20 in an effort to determine the cause of the discontinuous yielding. However, Laue X-ray back reflection

analysis was inconclusive due to the similarity in the diffraction patterns of single crystal B2 (cubic) and B27 (orthorhombic) structures. Differential scanning calorimetry (DSC) was performed from 300 K to 1475 K on the material taken from the distorted region of specimen #2, and an exothermic event at 455 K was observed that could be associated with the transformation from B27 phase to B2 phase. The B2 phase is the more stable phase at elevated temperature. DSC was also performed on an YCu single crystal not subjected to tensile or compression testing and on an YCu single crystal specimen that had been tensile tested. Neither of those DSC patterns displayed an exothermic event at 455 K, findings that are consistent with the conclusion that the discontinuous yielding was caused by transformation to the B27 phase induced by the high compressive stress. This issue requires further study before the cause of the discontinuous yielding can be determined with certainty.

7.4 $(Tb_{0.88}Dy_{0.12})Zn$ Fracture

Possible slip systems for the B2 structure include the $\{100\}<010>$, $\{101\}<010>$, $\{110\}<\bar{1}11>$, $\{110\}<\bar{1}10>$, $\{211\}<\bar{1}11>$, and $\{321\}<\bar{1}11>$. One or more of the three different tensile axis orientations used for the $(Tb_{0.88}Dy_{0.12})Zn$ specimens positioned each of these slip systems in an orientation where the resolved shear stress is high, affording opportunities for slip on every one of these slip systems. Since all of the $(Tb_{0.88}Dy_{0.12})Zn$ specimens failed by brittle fracture, we conclude that none of the likely slip systems in $(Tb_{0.88}Dy_{0.12})Zn$ is active.

7.5 YCu Slip

The results shown in Table 6 and Figures 18 and 19 clearly indicate that slip occurred in the single crystal YCu tensile test specimens. The angles between the slip lines marked on Figure 19 and angles measured on the minor faces of the YCu tensile test specimens were used to determine the planes that

were slipping in the YCu specimens. These angles are tabulated in Table 7.

By developing a three-dimensional model of the crystallographic planes with computer graphics software, it was possible to search for crystallographic planes that could produce the angles of intersection (Table 7 below) observed on the major and minor surfaces of the YCu tensile test specimens. All four likely slip planes for a B2 crystal (i.e. {100}, {110}, {211}, {321}) were checked in this way, and it was found that the angles of intersection of the (010) and (101) planes with the $(\bar{8}12)$ plane and the $(\bar{2}6\bar{1}\bar{1})$ plane matched all six angles in Table 7 within $\pm 1^{\circ}$. No such match was found for the {211} or {321} planes.

With the (010) and (101) planes identified as the apparent slip planes in the YCu tensile test specimens, the next step in the analysis was to determine the active slip directions on these slip planes. Likely slip directions in the (010) plane are <001> and <101>. The possible slip directions for the (101) plane are <010>, $<\bar{1}01>$, and $<\bar{1}11>$. Schmid's Law relates tensile stress to the shear stress resolved onto a particular slip plane and slip direction:

$$\tau = \sigma (\cos \phi)(\cos \lambda)$$

where τ = shear stress on a given slip plane, σ = the tensile stress on the sample, ϕ = the angle between the slip plane's normal vector and the tensile axis, and λ = the angle between the slip direction and the tensile axis. The $(\cos \phi)(\cos \lambda)$ term is often referred to as the Schmid factor. Orientations with a large Schmid factor are favored for slip since the shear stress (τ) available to move dislocations is directly proportional to the Schmid factor for a given tensile stress (σ) on the crystal.

A given slip system (e.g. the {101}<010>) contains several

individual planes (e.g. the (101), (110), ($\bar{1}$ 01), etc.), and each of those planes contains two or more possible slip directions (e.g. the [010], [001], etc.). Since the critical resolved shear stress (τ_{CRSS}) for slip is the same for every member of a given slip family, the particular plane and direction of that slip system that actually does slip as plastic flow begins in the tensile test will be the combination with the highest Schmid factor. Therefore, it should be possible to determine which slip directions are active on a given slip plane by calculating the Schmid factor for all possible slip directions on a given plane and noting whether the plane-direction combination that is observed to slip has the highest Schmid factor. If so, then that slip direction is a plausible candidate for an active slip direction on the plane in question. If not, then it is unlikely that that family of slip directions undergoes slip on the plane in question. Such calculations were performed for slip on the {100} family of planes to produce the values tabulated in Table 8 below. Table 8a shows the possible combinations of slip directions in the {010} family of planes; and the largest Schmid factor (0.381) occurs for the (010)[001] and for the (001)[010] slip systems. Since the slip plane analysis indicated that slip was occurring on the (010), finding that the (010)[001] system has the highest Schmid factor suggests that the <001> slip direction is a possibly active slip direction on the {010} family of planes.

However, when the same set of calculations is performed on the other candidate slip direction, the <011> family, for {010} slip, the largest Schmid factor (0.404) again occurs for the (010) plane, as shown in Table 8b. Thus, from this Schmid factor analysis, both the [001] and the [101] slip directions appear to be possible candidates for the slip direction on the {010}. However, the Burgers vector length is considerably shorter for the [001] than it is for the [101], suggesting

that the [001] slip direction is the more likely of the two. Also, in other B2 intermetallic systems, slip has been observed to occur preferentially along the <001> direction when the ordering energy of the compound is high. Since the electronegativity difference between Y and Cu is large (0.7 Pauling), the ordering energy for YCu is presumably large as well, which again suggests that the [001] direction is the more probable one for YCu slip on the {010} planes.

A similar Schmid factor analysis performed for the {101} slip planes in YCu (Table 9 below), indicates that slip is occurring in the [010] direction. In Table 9a, the Schmid factor for the [010](101) is the largest of the six values shown in Table 9a, indicating that the [010] is a plausible slip direction for the {101} planes. In Table 9b, the Schmid factor for the $[\bar{1}01](101)$ and the $[101](\bar{1}01)$ are the smallest of the six values in Table 9b, indicating that the <101> is an unlikely slip direction for the {101} planes. Finally, Table 9c shows that a Schmid factor of 0.292 for the $[\bar{1}11](101)$ is considerably smaller than the Schmid factors of other possible candidates in Table 9c, indicating that the <111> is an unlikely slip direction for the {101} planes.

From the foregoing Schmid factor analyses of the slip lines on the YCu tensile test specimen surfaces, we conclude that the {100}<010> and {110}<010> were the likely slip systems active during these tensile tests. This analysis by itself, however, does not definitively prove this conclusion. The correctness of this conclusion could be tested by tensile testing cylindrical single crystal specimens, by transmission electron microscope analysis of the Burgers vectors of dislocations in the test specimens, or by testing other crystal orientations. We chose to perform the last of these three alternatives by conducting the compression tests described above.

As Figure 18 shows, the yield stress for the YCu single

crystal tensile test specimens was ~45 MPa. If the value for σ in Schmid's Law is set at 45 MPa, τ_{CRSS} on each of these two slip systems can be calculated. For the {100}<010>, τ_{CRSS} was determined to be 17 MPa, and for the {110}<010>, τ_{CRSS} was determined to be 18 MPa. If these two slip systems are the only ones active in YCu, this material would have only three independent slip systems, and it would fail to meet the von Mises criterion of five independent slip systems for plasticity in a polycrystalline material. The [142] tensile axis orientation produces high Schmid factors for the {100}<010> and {110}<010> slip systems. If a second test could be performed on single crystal YCu with an orientation that produced a zero Schmid factor for these two slip systems, it might be possible to determine whether other, secondary slip systems are also active at room temperature (possibly with higher values of τ_{CRSS}). If additional slip system(s) were found to be active, the total number of independent slip systems in YCu could be sufficient to satisfy the von Mises criterion.

With this motivation, compression tests were performed on YCu single crystals oriented with [100] parallel to the compression axis. The high yield stresses observed in these specimens (Figure 20) indicate that no slip directions other than <100> will move in YCu, even at τ_{CRSS} values several times greater than the 17 to 18 MPa observed for the {100}<010> and {110}<010> slip systems. This finding further supports our conclusion that only <010> slip directions are active on the {100} and {110} planes.

To summarize this example, single crystal specimens of YCu intermetallic compound were tested in tension and in compression at room temperature, and single crystal specimens of $(Tb_{0.88}Dy_{0.12})Zn$ compound were tested in tension at room temperature.

- Single crystal tensile specimens of $(Tb_{0.88}Dy_{0.12})Zn$ with tensile axes parallel to <100>, <211>, and <111> all failed by brittle fracture.
- Single crystal YCu tensile specimens with a [142] tensile axis orientation elongated 6% to 8% before fracture, and the active slip systems in YCu in tension appear to be {100}<010> (τ_{CRSS} = 17 MPa) and {110}<010> (τ_{CRSS} = 18 MPa).
- Single crystal YCu specimens were compression tested with the <100> direction as the tensile axis. That orientation puts no resolved shear stress on either the {100}<010> or the {110}<010>, and these compression tests resulted in yield stresses of approximately 300 MPa followed by what is believed to be a stress-induced transformation to the B27 crystal structure.

Table 5.
Ultimate Tensile Strengths and Elongation of $(Tb_{0.88}Dy_{0.12})Zn$ Single Crystal Tensile Test Specimens

Tensile Axis Orientation	Tensile Strength (MPa)	Elongation (%)
[100]	130	nil
[100]	116	nil
[100]	105	nil
[100]	46	nil
[211]	226	nil
[211]	197	nil
[111]	190	nil
[111]	174	nil

Table 6.
Ultimate Tensile Strengths and Elongation of YCu Single Crystal Tensile Test Specimens

Tensile Axis Orientation	Tensile Strength (MPa)	Elongation (%) at Fracture
[142]	70	9.5
[142]	75	7.6
[142]	73	8.2
[142]	88	8.9

Table 7.
Angles of Slip Lines on the Surfaces of YCu Single Crystal Tensile Test Specimens

	Major Face	Minor Face
Acute Angle of First Set of Slip Lines with Tensile Axis	62°	83°
Acute Angle of Second Set of Slip Lines with Tensile Axis	31°	41°
Acute Angle Between the Two Slip Lines	87°	55°

Table 8.
Schmid Factors for Candidate Slip Directions on the {010} Family of Slip Planes

8a) The <010> slip direction

Slip Direction	Slip Plane	Schmid Factor
[010]	(100)	0.190
[001]	(100)	0.095
[100]	(010)	0.190
[001]	(010)	0.381
[100]	(001)	0.095
[010]	(001)	0.381

8b) The <011> slip direction

Slip Direction	Slip Plane	Schmid Factor
[011]	(100)	0.202
$[01\bar{1}]$	(100)	0.067
$[\bar{1}01]$	(010)	0.134
[101]	(010)	0.404
[110]	(001)	0.337
$[\bar{1}10]$	(001)	0.202

Table 9.
Schmid Factors for Candidate Slip Directions on the {101} Family of Slip Planes

9a) The <001> slip direction

Slip Direction	Slip Plane	Schmid Factor
[001]	(110)	0.337
[001]	$(\bar{1}10)$	0.202
[010]	(101)	0.404
[010]	$(\bar{1}01)$	0.135
[100]	(011)	0.202
[100]	$(01\bar{1})$	0.067

9b) The <110> slip direction

Slip Direction	Slip Plane	Schmid Factor
$[\bar{1}10]$	(110)	0.357
[110]	$(\bar{1}10)$	0.357
$[\bar{1}01]$	(101)	0.071
[101]	$(\bar{1}01)$	0.071
$[01\bar{1}]$	(011)	0.286
[011]	$(01\bar{1})$	0.286

9c) The <111> slip direction

Slip Direction	Slip Plane	Schmid Factor
$[\bar{1}\,11]$	(110)	0.486
$[\bar{1}\,1\bar{1}]$	(110)	0.097
$[\bar{1}\,11]$	(101)	0.292
$[11\bar{1}]$	(101)	0.175
[111]	$(\bar{1}\,10)$	0.408
$[11\bar{1}]$	$(\bar{1}\,10)$	0.175
[111]	$(\bar{1}\,01)$	0.136
$[\bar{1}\,1\bar{1}]$	$(\bar{1}\,01)$	0.019
$[11\bar{1}]$	(011)	0.350
$[\bar{1}\,\bar{1}\,\bar{1}]$	(011)	0.117
$[\bar{1}\,11]$	$(01\bar{1})$	0.195
[111]	$(01\bar{1})$	0.273

Figure 22 shows a comparison of the anisotropy factor, $A^{-1/2}$, versus the Poisson ratio for YAg, YCu, and DyCu as well as for body-centered cubic (bcc) transition metals, ionic compounds, and non-RM intermetallic compounds for comparison. The RM intermetallic compounds, YAg, YCu, and DyCu, pursuant to the invention are more isotropic in having an elastic anisotropy value $A^{-1/2}$ of about 1 (e.g. 0.8 to 1.0) compared with the strong anisoptropy (e.g. $A^{-1/2}$ greater than 1.2 or less than 0.75) of the ionic compounds and the non-RM intermetallic compounds shown in Figure 22. For information purposes, the elastic anisotropy A is represented by $A = 2c_{44}/(c_{11}-c_{12})$ where Cu_{11}, C_{12}, and C_{44} are three components of the stiffness tensor which are associated with the tensile stress along the cube axis (C_{11}), the shear stress in cube plane (C_{12}), and compressive stress (C_{44}).

Articles of manufacture pursuant to the invention include, but are not limited to, an engine component for an internal combustion engine of a vehicle including automobiles and trucks, a component for a gas turbine engine, a load-bearing structural component for a vehicle including automobiles, trucks and aircraft, valve, nozzle, separator, a component of a pump, boiler tube, a die for both cold and hot pressing, forging or otherwise shaping a metallic or other material, a component of mining or petroleum recovery equipment, a damping component to reduce vibrations, a clad component, a dental component, component of a medical device, jewelry (particularly black gold formed by oxide layers on the RM material where M = Au), catalyst, getter, diffusion barrier component, an electrical component such as for example a resistor, an electrical contact, an electrical sensor, a battery component, micro-electro-mechanical system (MEMS), a magnetic component such as, for example, a hard or soft magnet, magnetoresistance devices, magnetorestrictors, transducers, hydrogen storage materials, membrane for hydrogen separation and/or purification, coatings, superconductors, metallic mirrors, antibacterial agents, and large neutron absorption cross-section materials containing Sm, Eu, Gd, and/or Dy for nuclear applications, such as control rods, burnable poisons, and shutdown and safety devices for nuclear reactors and nuclear shielding materials.

The present also involves a method of making an article of manufacture by plastically deforming a body comprising an intermetallic compound described above; for example, wherein the compound is selected from the group consisting of an RM compound and a higher order compound thereof having a CsCl-type ordered crystal structure wherein R is one or more rare earth elements and M is one or more non-rare earth metals and is also selected from the group consisting of a M'M compound and a higher order compound thereof having a CsCl-type ordered

crystal structure wherein M' and M are one or more different non-rare earth metals.

The following examples are offered to further illustrate but not limit the invention.

As an example of the ductility achievable by practice of the invention, a specimen of YAg intermetallic compound was deformed by rolling at room temperature from an initial thickness of 0.094 inch (2.39 mm) to a final thickness of 0.011 inch (0.28 mm). This deformation is an 88% reduction by cold rolling. The plastic deformation was conducted with no stress relief annealing to provide for recrystallization. The specimen strip showed only a modest amount of edge cracking of the sort typically seen in cold rolled copper or steel. The central 80% of the rolled specimen strip was free of cracks.

As another illustrative example, a specimen of YCu intermetallic compound was deformed by rolling at elevated temperature (700 degrees C) from an initial thickness of 0.35 inch (9.0 mm) to a final thickness of 0.079 inch (2.0 mm). This deformation is a 78% reduction by hot rolling. The specimen was enclosed in a Ta-lined stainless steel can to prevent oxidation of the surface of the YCu. After hot rolling, the specimen was cold rolled an additional 15% to a final thickness of 0.067 inch (1.7 mm); the cold rolled specimen strip was 5.3 inches (135 mm) long and 0.79 inch (20 mm) wide. When the specimen strip was removed from the stainless steel can, it was almost completely free of any edge cracks. A few very small edge cracks approximately 0.1 inch (2.5 mm) deep were visible; the center section of the specimen strip had no cracks or flaws at all.

Although the invention has been described in terms of specific embodiments thereof, it is not intended to be limited thereto but rather only to the extent set forth hereafter in the appended claims.

CLAIMS

WE CLAIM

1. Article of manufacture fabricated of an intermetallic compound comprising R and M having a CsCl-type ordered crystal structure wherein R is one or more rare earth elements and M is one or more non-rare earth metals and having a tensile elongation of at least about 5% prior to fracture when tensile tested at room temperature in ambient air.

2. The article of manufacture selected from a compound represented by RM and a higher order compound thereof selected from (R,R')M, R(M,M'), (R,R')(M,M') and (R,R'...R^n)(M,M'...M^n), where the prime designates a different R or M element from the non-prime R or M and where n can be 3, 4 or more and designates a different R or M element from the other R or M elements of the compound.

3. The article of manufacture of claim 1 wherein said R element is selected from the group consisting of Sc, Y, La, Ce, Pr, Nd, Pm, Sm, Eu, Gd, Tb, Dy, Ho, Er, Tm, Yb, and Lu.

4. The article of manufacture of claim 1 wherein said M metal is selected from at least one late transition metal and Group I, II, or III metal of the Periodic Table.

5. The article of manufacture of claim 2 wherein said M element is selected from the group consisting of Mg, Al, Co, Ni, Cu, Zn, Ru, Rh, Pd, Ag, Cd, In, Ir, Pt, Au, Hg, and Tl.

6. The article of manufacture of claim 5 where said M element is selected from a metal or non-metal not included in claim 4 and whose concentration is limited to the maximum solid solubility of said metal or non-metal in said compound such that said compound retains said crystal structure.

7. The article of manufacture of claim 1 having a tensile elongation of at least about 10% prior to fracture when tensile tested at room temperature in ambient air.

8. The article of manufacture of claim 1 comprising an engine component for an internal combustion engine of a vehicle.

9. The article of manufacture of claim 1 comprising a component for a gas turbine engine.

10. The article of manufacture of claim 1 comprising a load-bearing structural component for a vehicle.

11. The article of manufacture of claim 1 comprising a die.

12. The article of manufacture of claim 1 comprising a component of mining or petroleum recovery equipment.

13. The article of manufacture of claim 1 comprising a damping component to reduce vibrations.

14. The article of manufacture of claim 1 comprising a clad component.

15. The article of manufacture of claim 1 comprising a dental component.

16. The article of manufacture of claim 1 comprising jewelry.

17. The article of manufacture of claim 1 comprising a catalyst.

18. The article of manufacture of claim 1 comprising a getter.

19. The article of manufacture of claim 1 comprising a diffusion barrier component.

20. The article of manufacture of claim 1 comprising an electrical component.

21. The article of manufacture of claim 1 comprising a magnetic component.

22. The article of manufacture of claim 1 comprising a valve.

23. The article of manufacture of claim 1 comprising a nozzle.

24. The article of manufacture of claim 1 comprising a separator.

25. The article of manufacture of claim 1 comprising a component of a pump.

26. The article of manufacture of claim 1 comprising a boiler tube.

27. The article of manufacture of claim 1 comprising a component of a component of a medical device.

28. The article of manufacture of claim 1 comprising a large neutron absorption cross-section material.

29. The article of manufacture of claim 1 comprising a hydrogen

storage member.

30. The article of manufacture of claim 1 comprising a membrane for hydrogen separation or purification.

31. The article of manufacture of claim 1 comprising a coating.

32. The article of manufacture of claim 1 comprising a superconductor.

33. The article of manufacture of claim 1 comprising a metallic mirror.

34. The article of manufacture of claim 1 comprising an antibacterial agent.

35. The article of manufacture of claim 1 comprising black gold jewelry having an oxide layer on the RM material where M is Au.

36. Article of manufacture fabricated of an intermetallic compound comprising M' and M having a CsCl-type ordered crystal structure wherein M' and M are one or more different non-rare earth metals having a tensile elongation of at least about 5% prior to fracture when tensile tested at room temperature in ambient air.

37. The article of manufacture of claim 36 comprising an engine component for an internal combustion engine of a vehicle.

38. The article of manufacture of claim 36 comprising a component for a gas turbine engine.

39. The article of manufacture of claim 36 comprising a load-bearing structural component for a vehicle.

40. The article of manufacture of claim 36 comprising a die.

41. The article of manufacture of claim 36 comprising a component of mining or petroleum recovery equipment.

42. The article of manufacture of claim 36 comprising a damping component to reduce vibrations.

43. The article of manufacture of claim 36 comprising a clad component.

44. The article of manufacture of claim 36 comprising a dental component.

45. The article of manufacture of claim 36 comprising jewelry.

46. The article of manufacture of claim 36 comprising a catalyst.

47. The article of manufacture of claim 36 comprising a getter.

48. The article of manufacture of claim 36 comprising a diffusion barrier component.

49. The article of manufacture of claim 36 comprising an electrical component.

50. The article of manufacture of claim 36 comprising a magnetic component.

51. The article of manufacture of claim 36 comprising a valve.

52. The article of manufacture of claim 36 comprising a nozzle.

53. The article of manufacture of claim 36 comprising a

separator.

54. The article of manufacture of claim 36 comprising a component of a pump.

55. The article of manufacture of claim 36 comprising a boiler tube.

56. The article of manufacture of claim 36 comprising a component of a component of a medical device.

57. The article of manufacture of claim 36 comprising a large neutron absorption cross-section material.

58. The article of manufacture of claim 36 comprising a hydrogen storage member.

59. The article of manufacture of claim 36 comprising a membrane for hydrogen separation or purification.

60. The article of manufacture of claim 36 comprising a coating.

61. The article of manufacture of claim 36 comprising a superconductor.

62. The article of manufacture of claim 36 comprising a metallic mirror.

63. The article of manufacture of claim 36 comprising an antibacterial agent.

64. The article of manufacture of claim 36 comprising black gold jewelry having an oxide layer on the M'M material where M' or M is Au.

65. A method of making an article of manufacture, comprising plastically deforming a body comprising an intermetallic compound comprising R and M having a CsCl-type ordered crystal structure wherein R is one or more rare earth elements and M is one or more non-rare earth metals.

66. A method of making an article of manufacture, comprising plastically deforming a body comprising an intermetallic compound comprising M' and M having a CsCl-type ordered crystal structure wherein M' and M are one or more different non-rare earth metals.

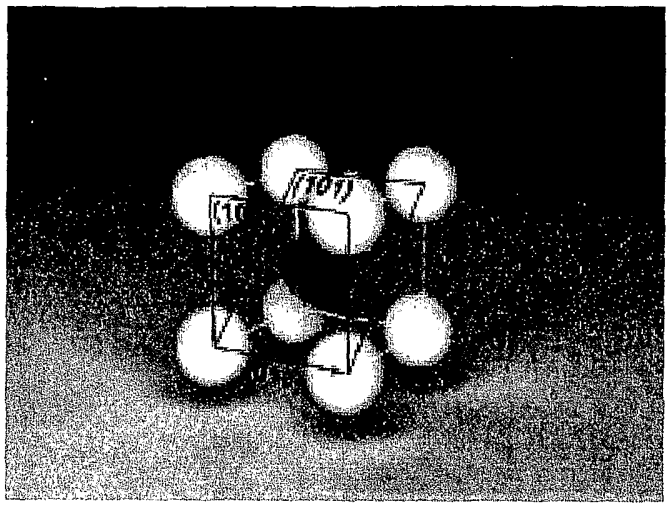


Figure 1

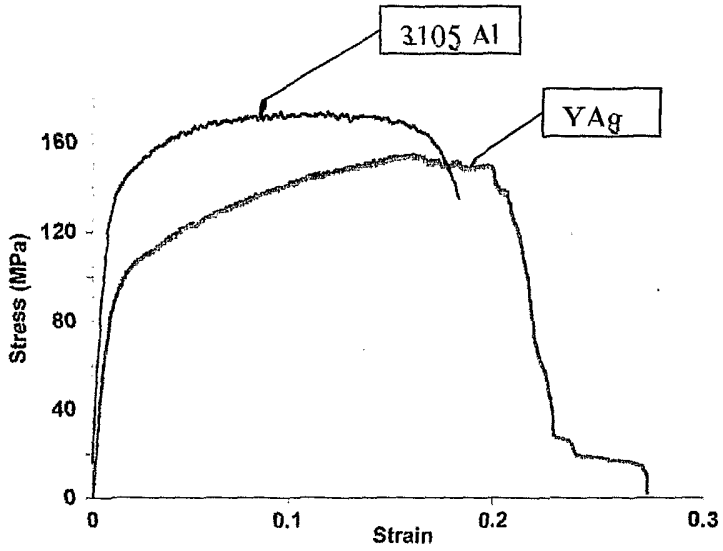


Figure 2

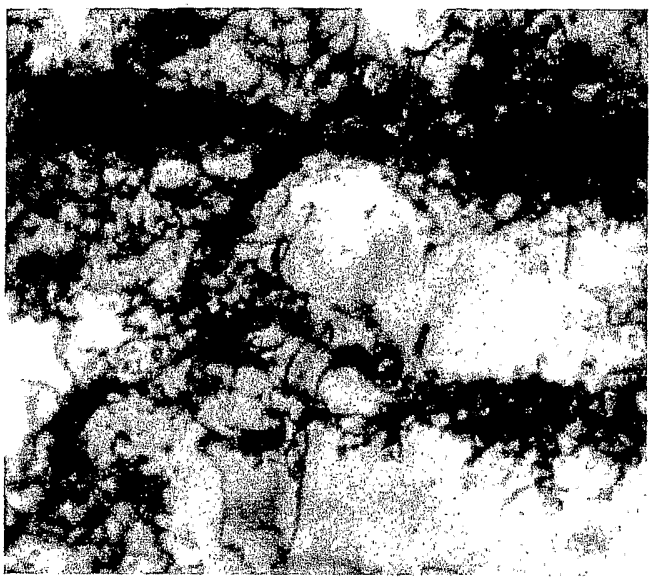


Figure 3

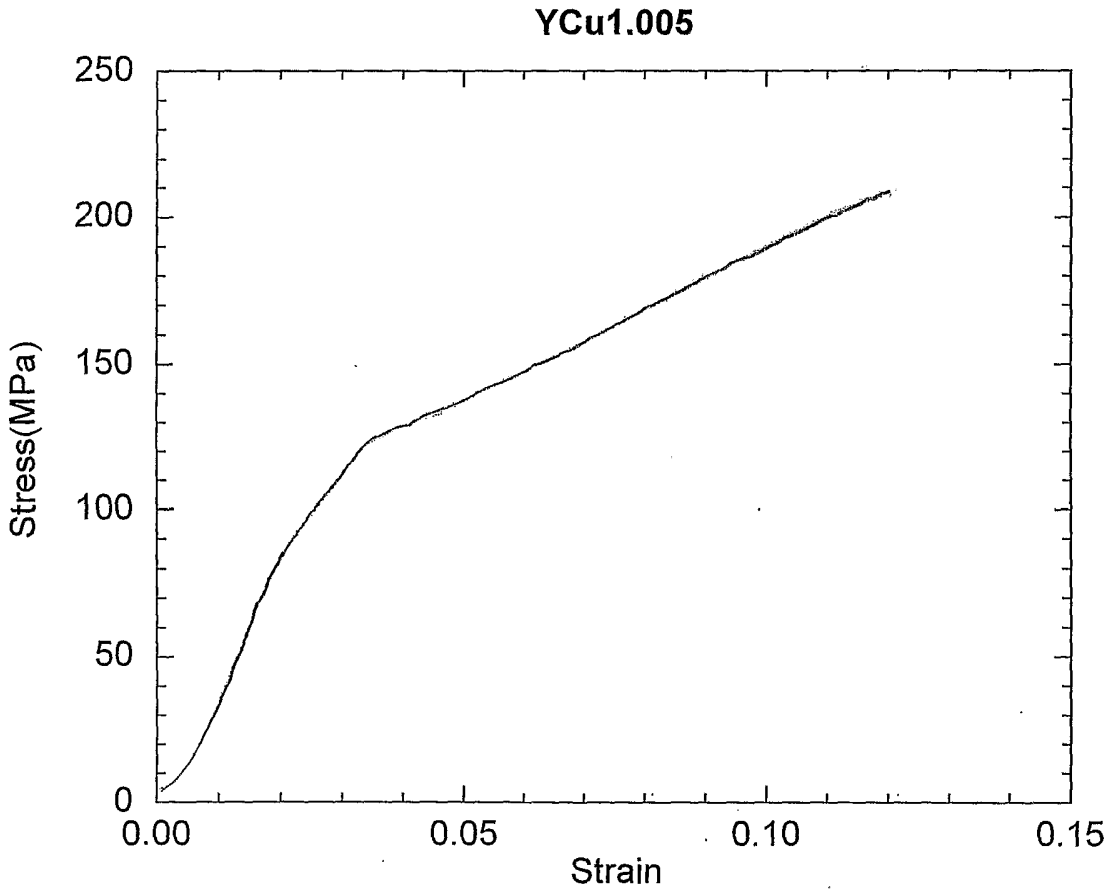


Figure 4

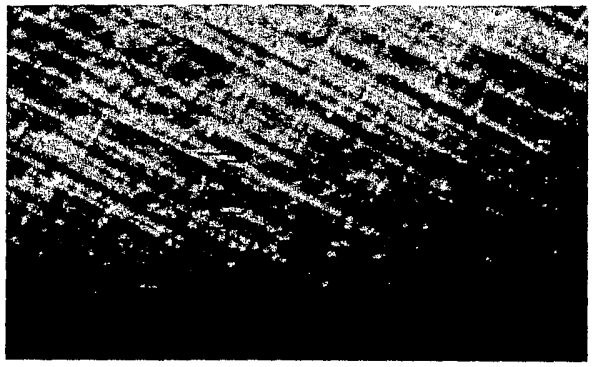


Figure 5

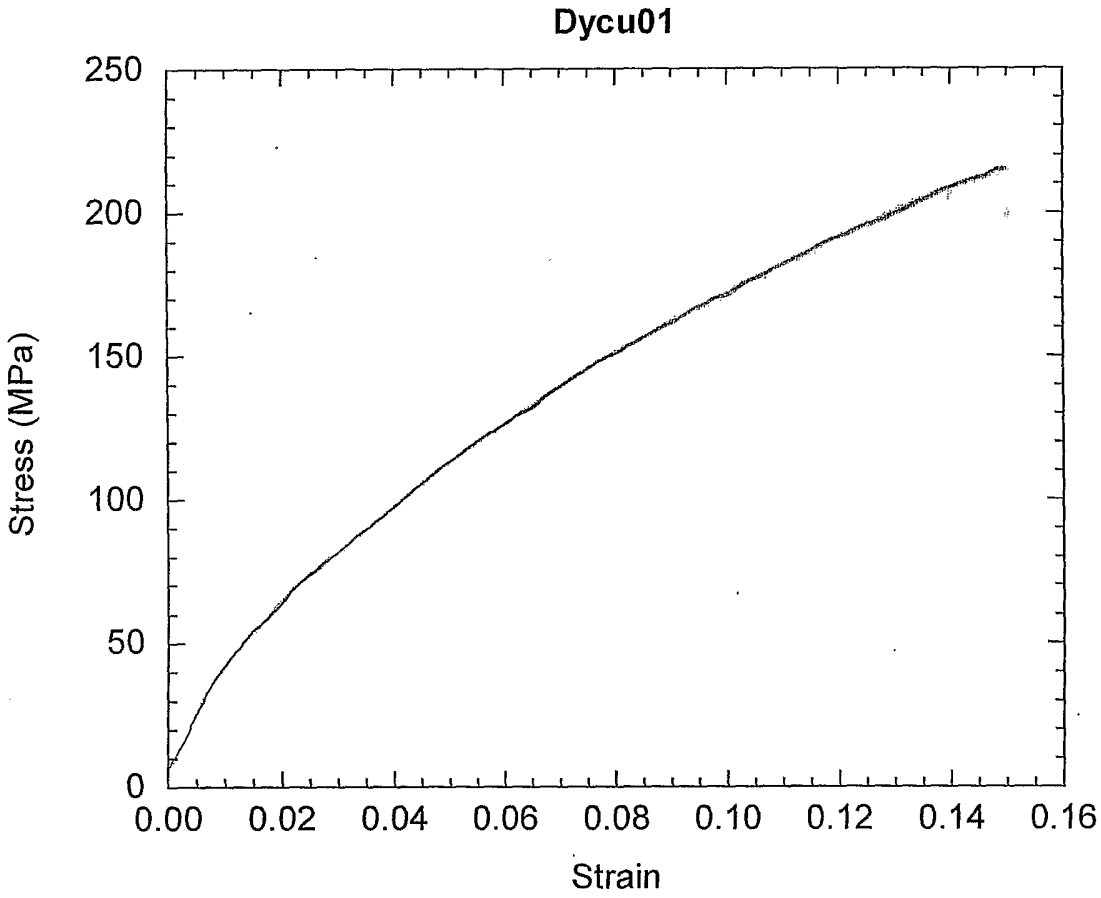


Figure 6

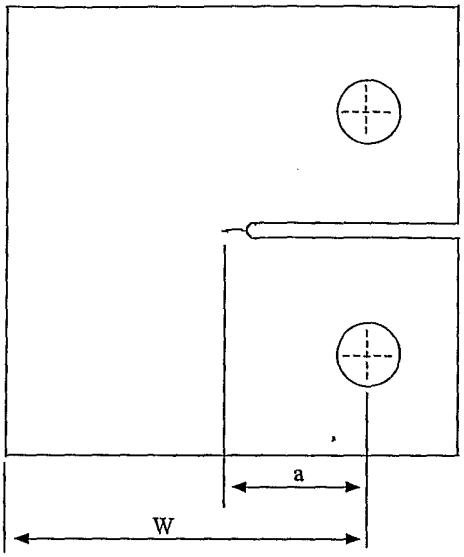


Figure 8

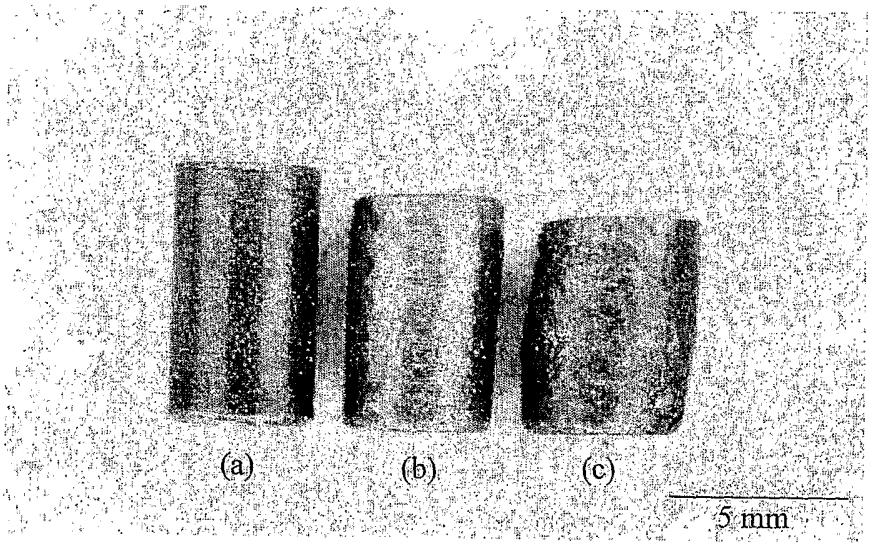


Figure 7

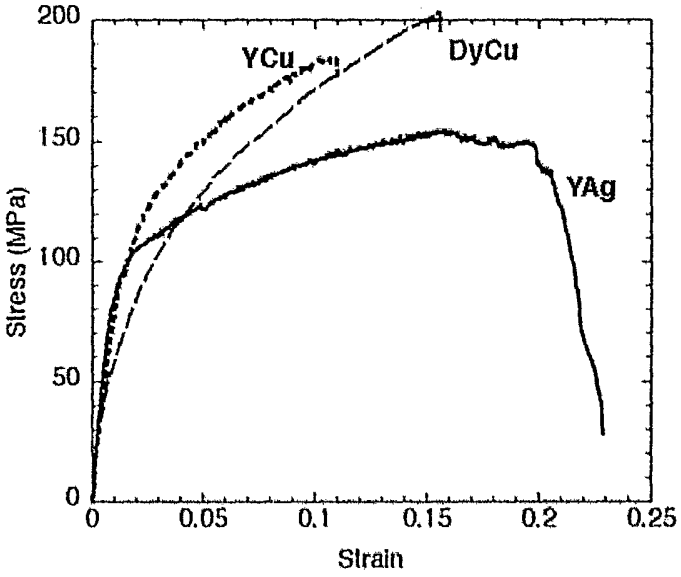

200
150
100
50
0
Stress (MPa)
0
0.05
0.1
0.15
0.2
0.25
Strain
YCu
DyCu
YAg

Figure 9

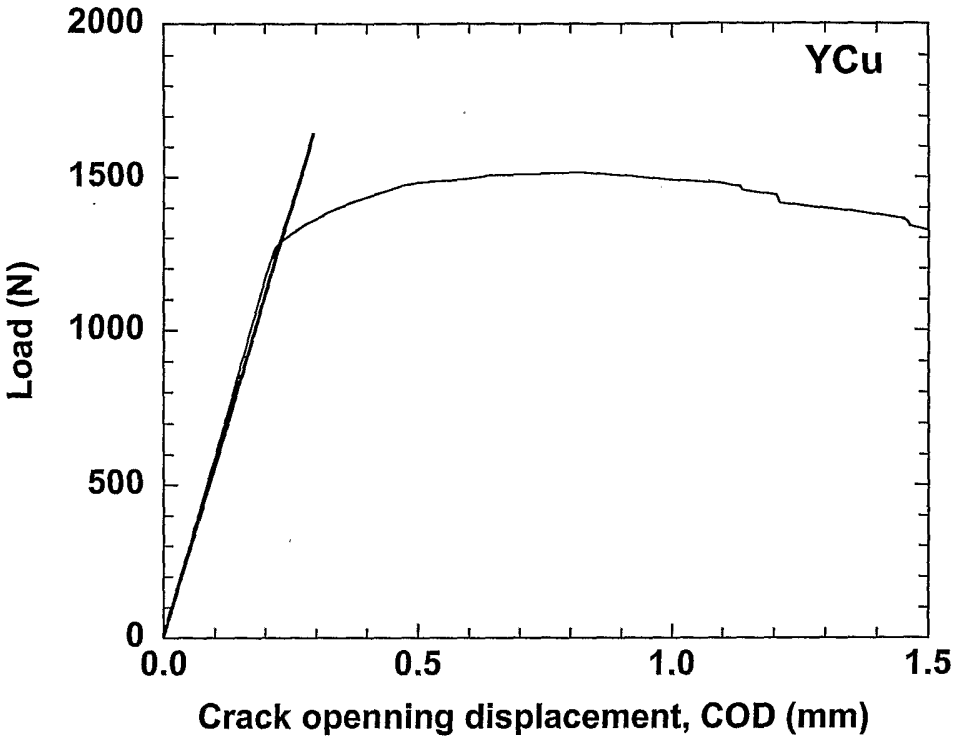

YCu
2000
1500
1000
500
0
Load (N)
0.0
0.5
1.0
1.5
Crack openning displacement, COD (mm)

Figure 10

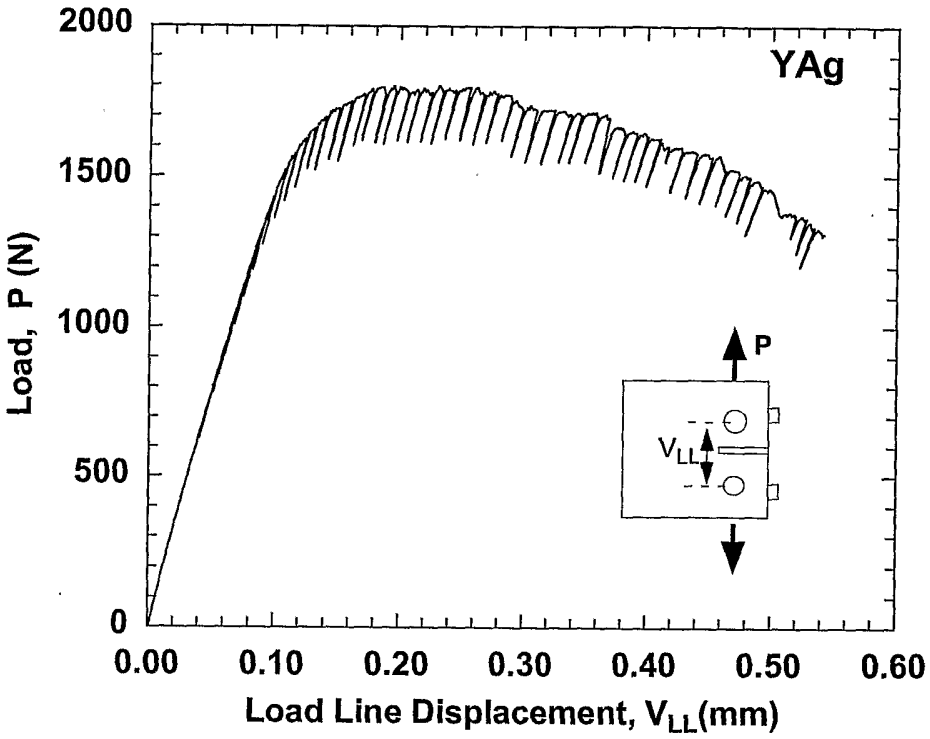

YAg
2000
1500
1000
500
0
Load, P (N)
0.00
0.10
0.20
0.30
0.40
0.50
0.60
Load Line Displacement, V_{LL}(mm)
P
V_{LL}

Figure 11

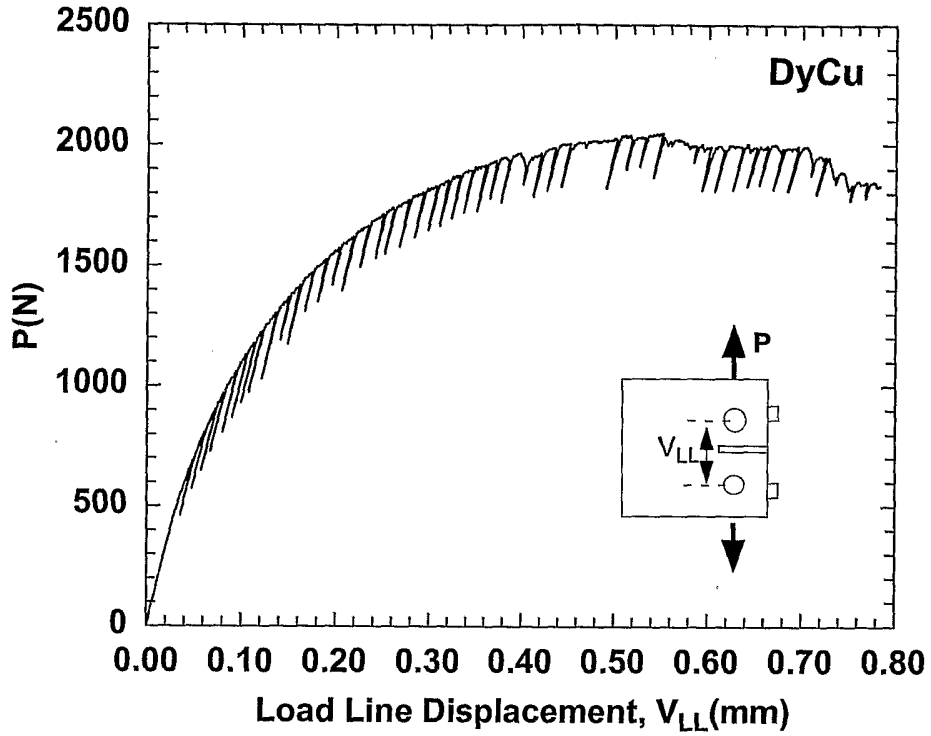

2500
2000
1500
1000
500
0
P(N)
DyCu
P
V_{LL}
0.00 0.10 0.20 0.30 0.40 0.50 0.60 0.70 0.80
Load Line Displacement, V_{LL}(mm)

Figure 12

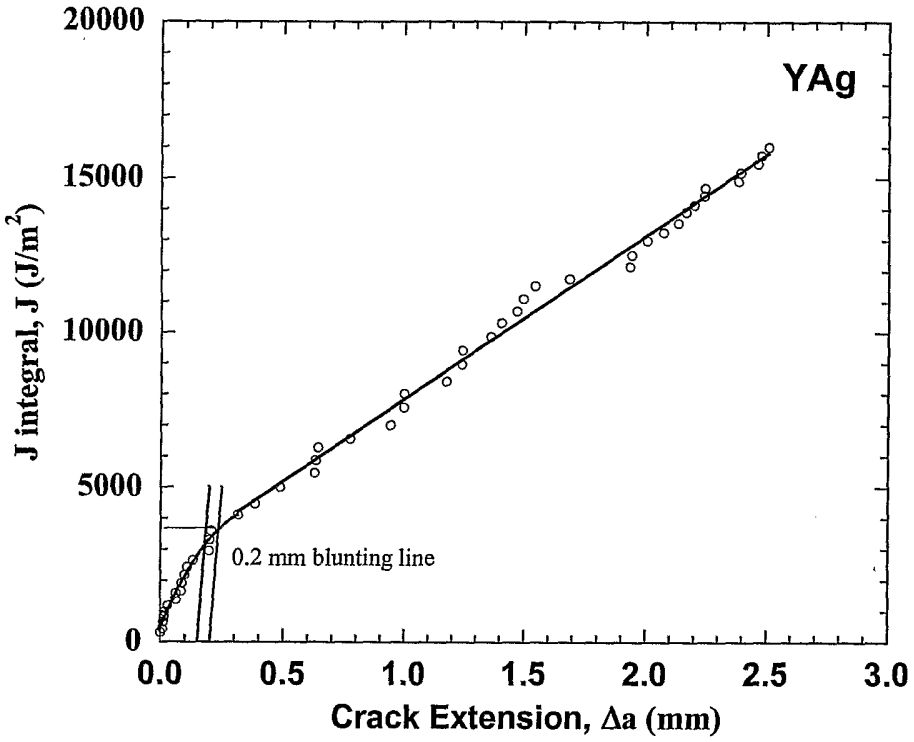

20000
15000
10000
5000
0
J integral, J (J/m^2)
YAg
0.2 mm blunting line
0.0
0.5
1.0
1.5
2.0
2.5
3.0
Crack Extension, Δa (mm)

Figure 13

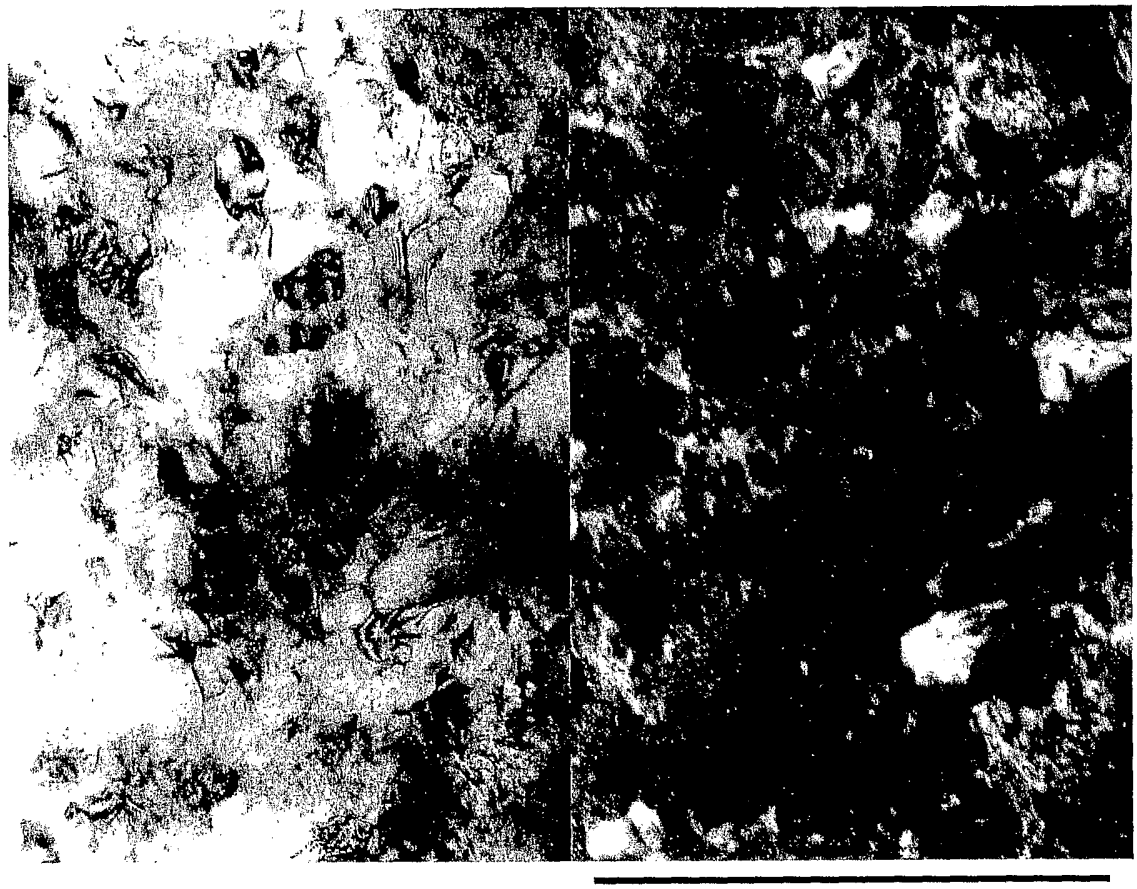


Figure 14a

Figure 14b

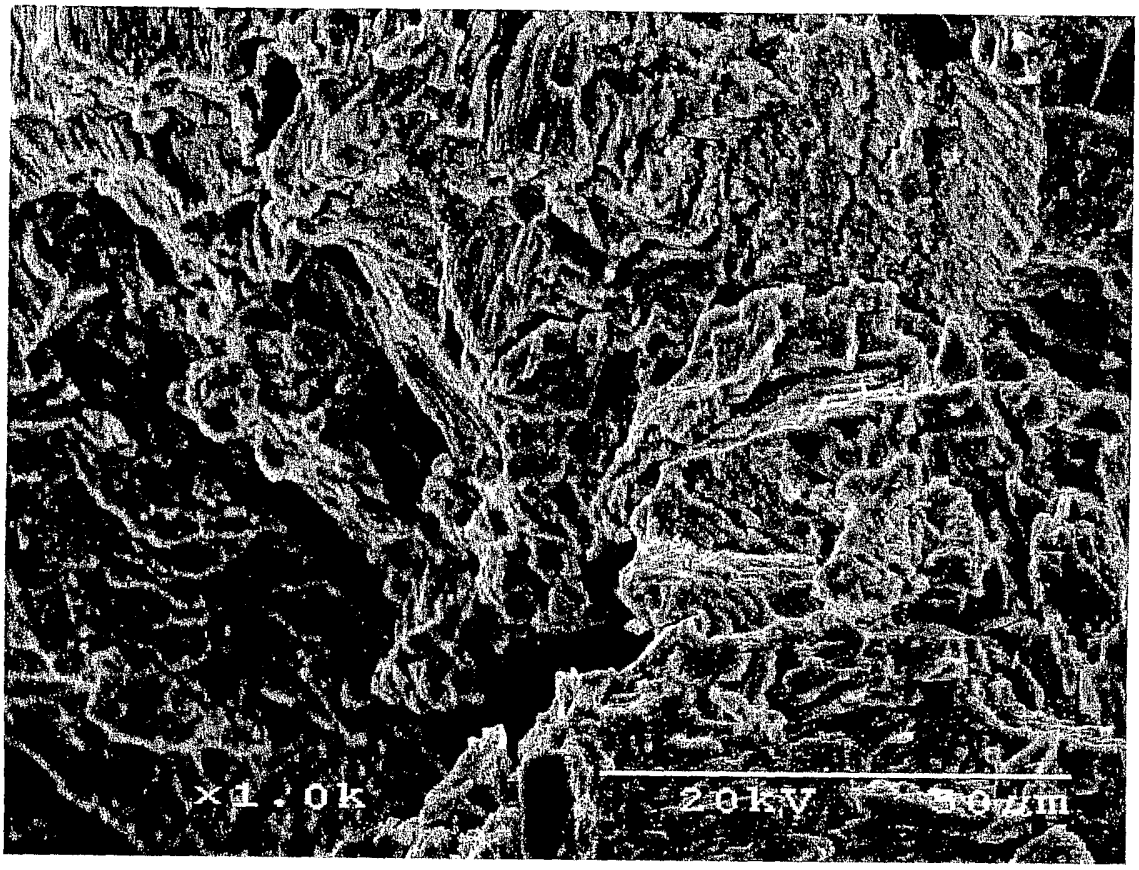


Figure 15

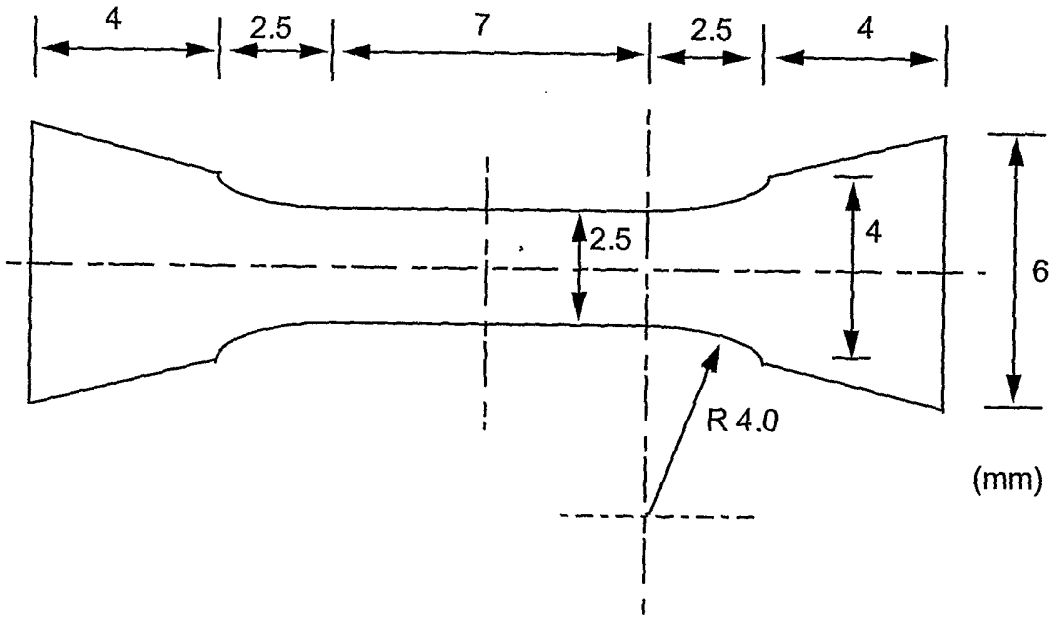


Figure 16

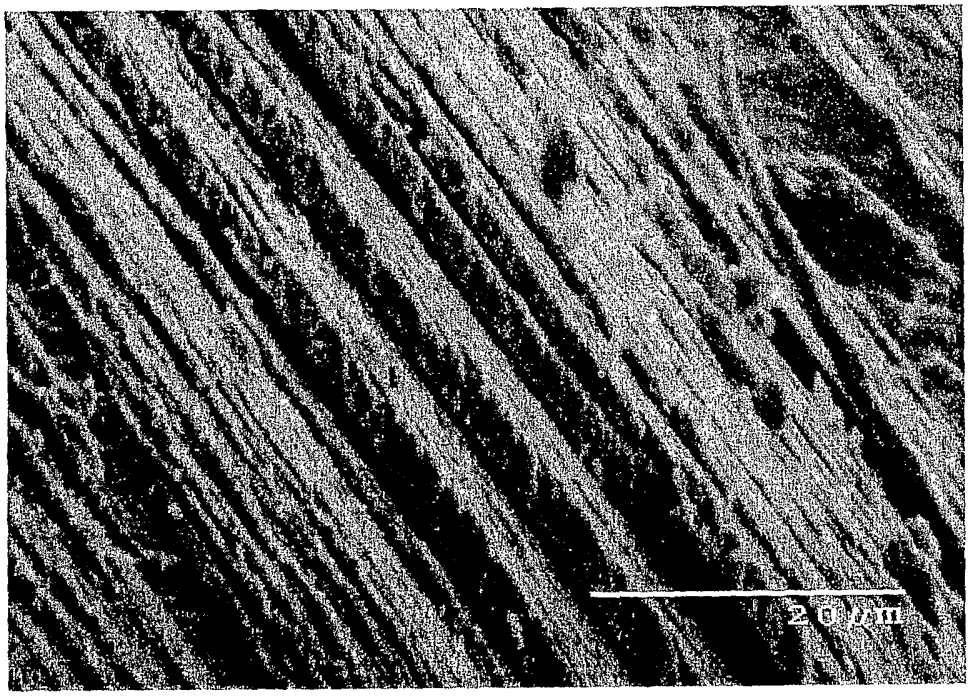


Figure 17

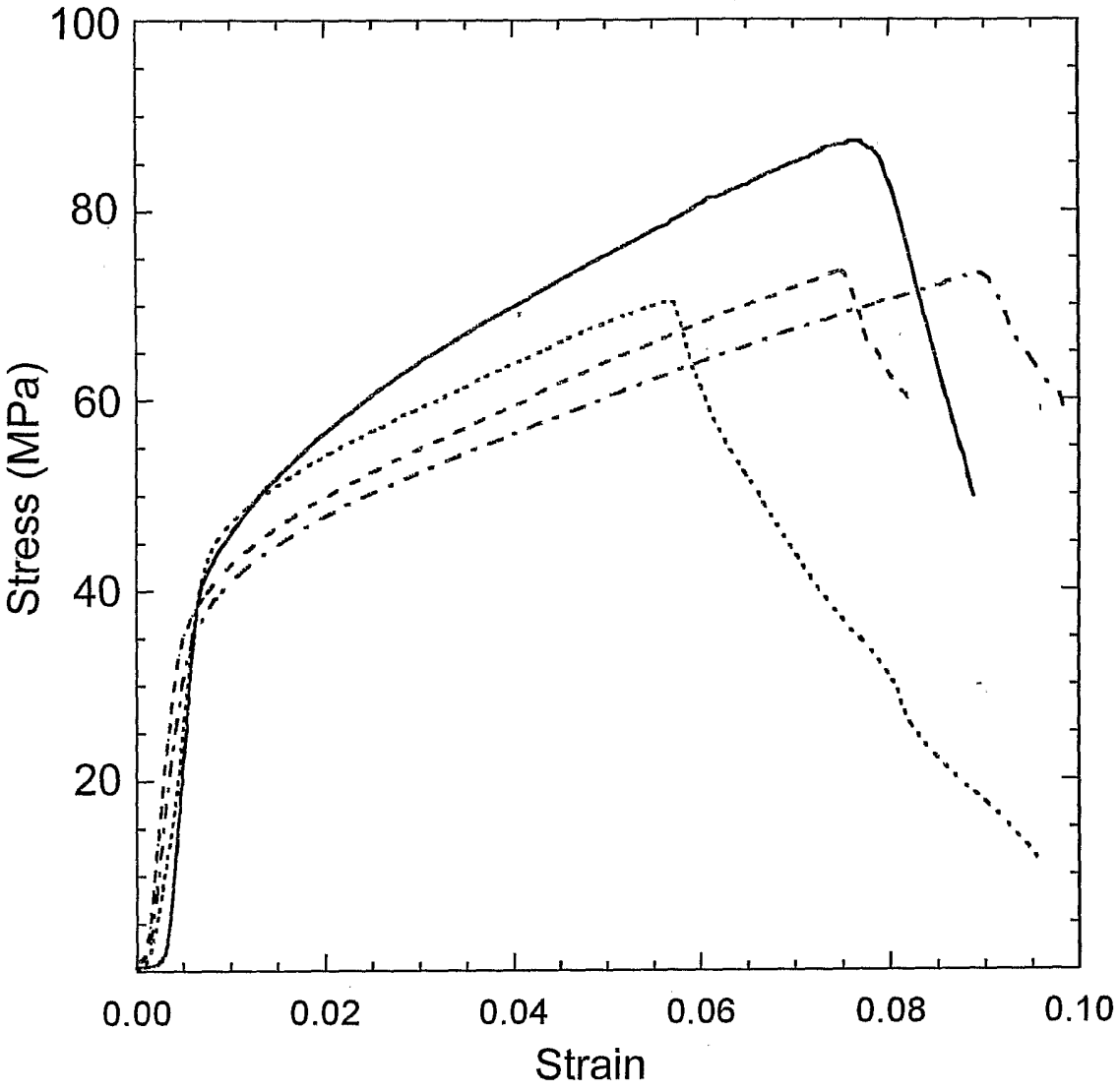


Figure 18

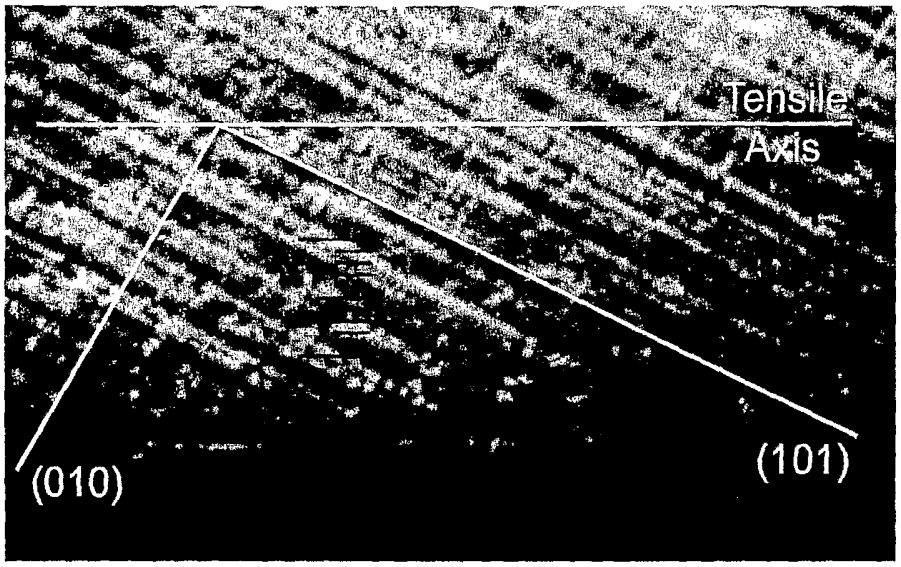


Figure 19

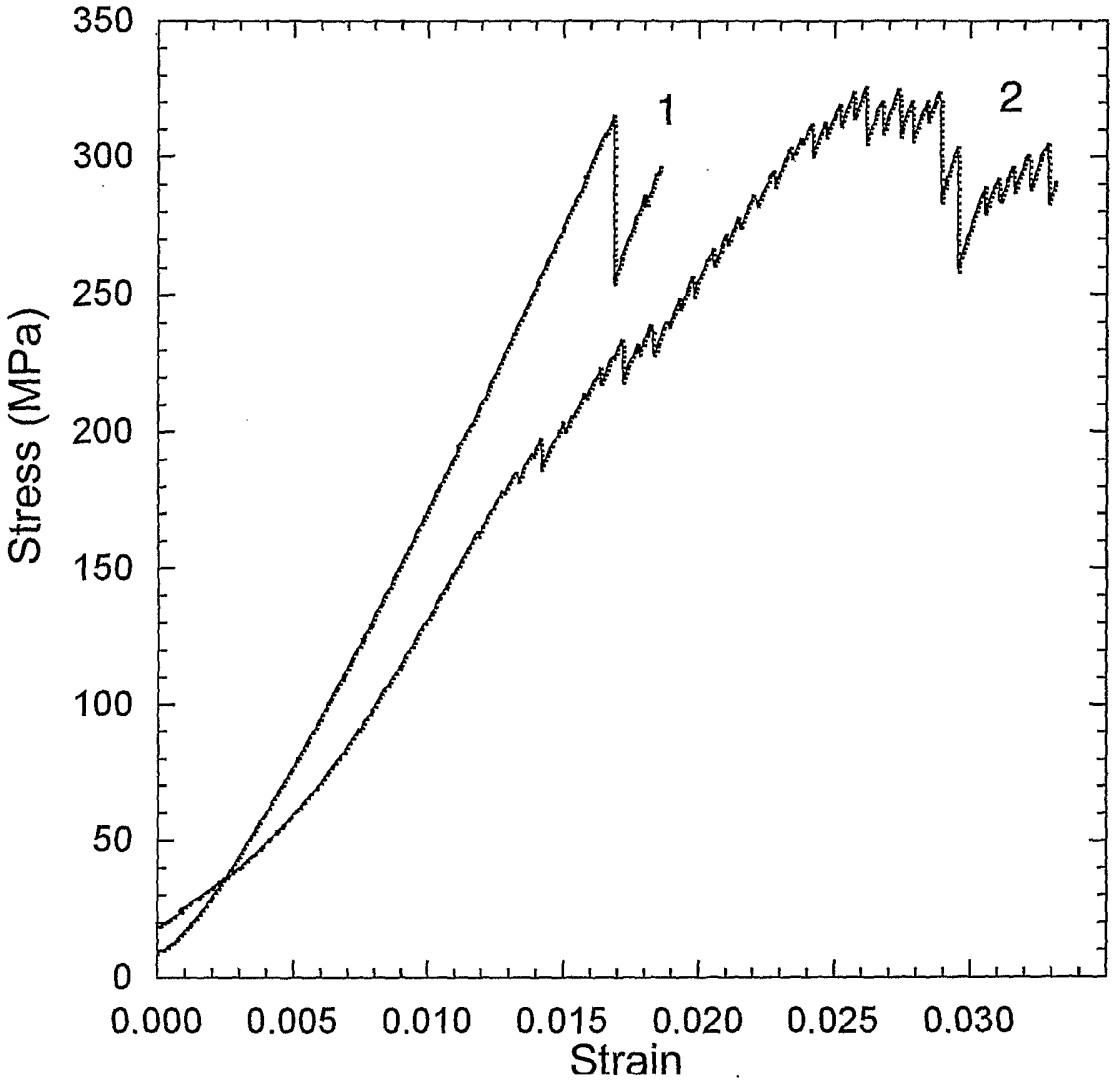

350
300
250
200
150
100
50
0
Stress (MPa)
0.000
0.005
0.010
0.015
0.020
0.025
0.030
Strain
1
2

Figure 20

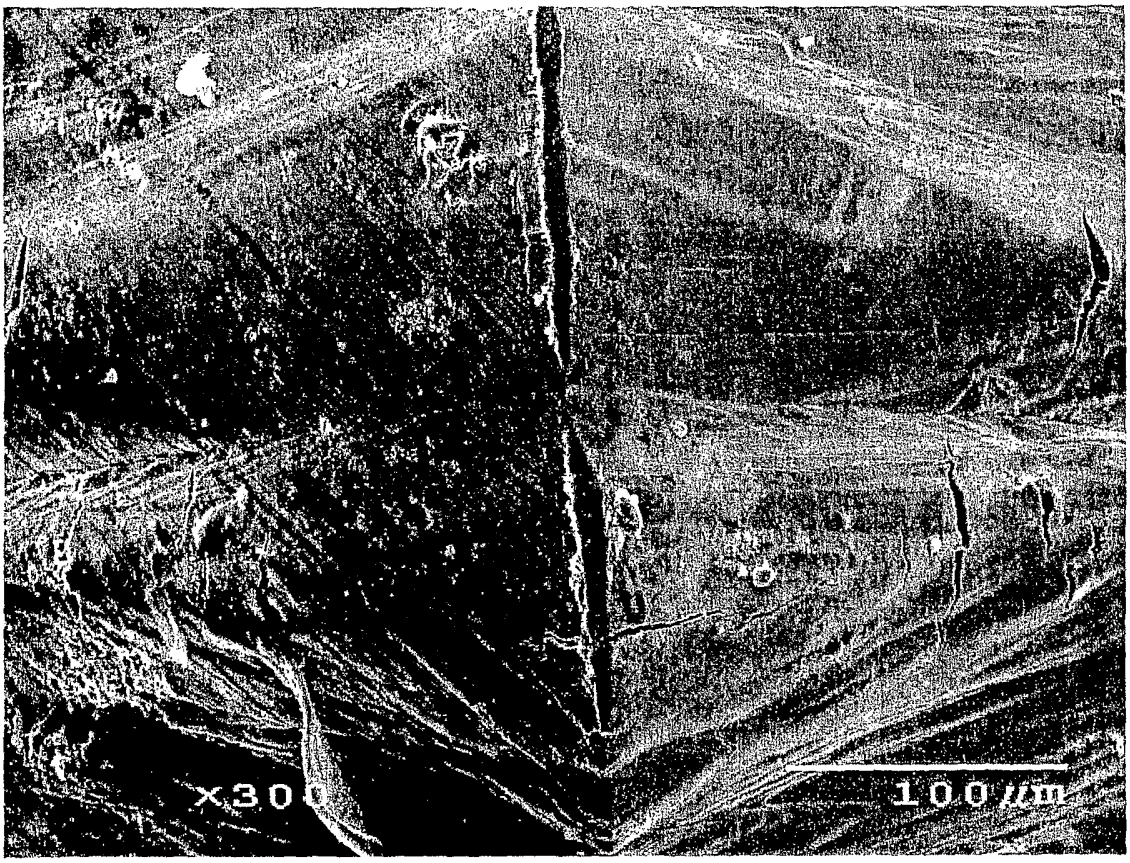


Figure 21

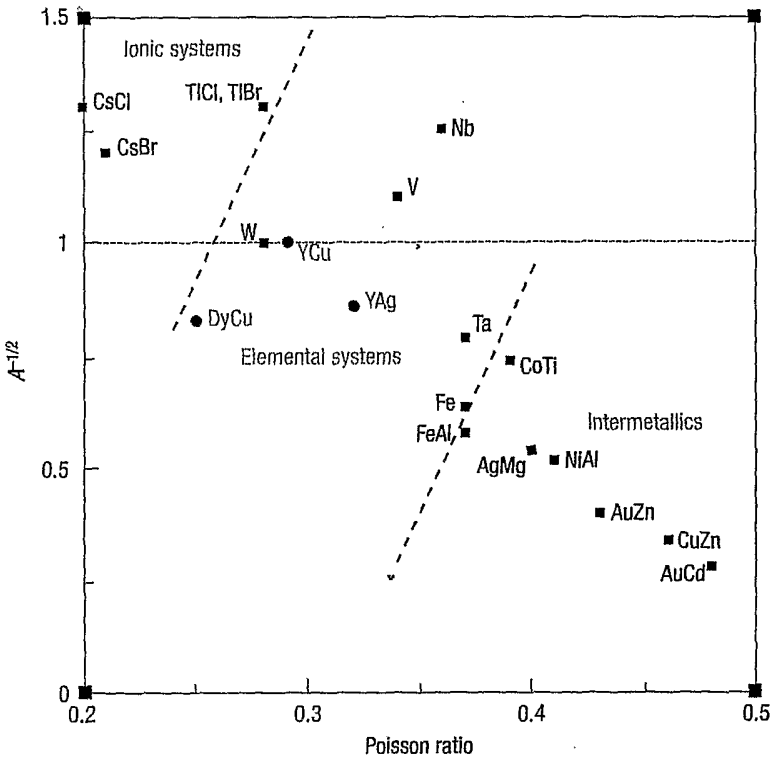

1.5
1
0.5
0
0.2
0.3
0.4
0.5
Poisson ratio
A-1/2
Ionic systems
CsCl
CsBr
TlCl, TlBr
Nb
V
W
YCu
YAg
DyCu
Ta
CoTi
Elemental systems
Fe
FeAl
Intermetallics
AgMg
NiAl
AuZn
CuZn
AuCd

Figure 22